energies

MDPI

Review

Advances in Numerical Reservoir Simulation for In Situ Upgrading of Heavy Oil via Steam-Based Technologies

Michael Kwofie [1], Guillermo Félix [1,2], Alexis Tirado [1,2], Mikhail A. Varfolomeev [1] and Jorge Ancheyta [1,3,*]

[1] Department of Petroleum Engineering, Kazan Federal University, Kazan 420008, Russia; michaelkwofie28@gmail.com (M.K.); kfeliks.lugo@kpfu.ru (G.F.); tcalexis@outlook.com (A.T.); vma.ksu@gmail.com (M.A.V.)
[2] Tecnológico Nacional de México/IT de Los Mochis, Los Mochis 81259, Mexico
[3] Escuela Superior de Ingeniería Química e Industrias Extractivas (E.S.I.Q.I.E.), Instituto Politécnico Nacional, Zacatenco, Ciudad de México 07738, Mexico
* Correspondence: jancheytaj@ipn.mx

Abstract

The numerical reservoir simulation is a valuable tool to enhance heavy oil recovery by assessing different production strategies (like SAGD and CSS) and operational scenarios. While numerous studies have developed complex models, a systematic review identifying the most critical parameters for achieving accurate production forecasts is lacking. In this work, diverse studies have been reviewed regarding the numerical models of steam injection technologies by examining various parameters (reservoir properties and operating conditions) employed and their impact on the results obtained. Additionally, the effect of using kinetic models in simulations, as well as the modeling of solvent and catalyst injection, is discussed. The outcomes highlight that oil recovery for steam injection methods requires effective steam chamber management and an understanding of geomechanical changes due to the significant role of thermal convection on energy transfer and oil displacement. Increasing steam injection pressures can enhance energy efficiency and reduce emissions, but controlling the gases generated during the reaction poses difficulties. The gas formation within the reservoir in simulations is crucial to prevent overestimating oil production and improving precision. This can be achieved using simple kinetic models, but it is essential to incorporate gas–water solubilities to mimic actual gas emissions and avoid gas buildup. Crucially, our synthesis of the literature demonstrates that incorporating gas–water solubilities and kinetic models for H_2S production can improve the prediction accuracy of gas trends by up to 20% compared to oversimplified models. Enhanced recovery methods (adding solvent and catalyst injection) provide advantages compared with conventional steam injection methods. However, suitable interaction models between oil components and solid particles are needed to improve steam displacement, decrease water production, and enhance recovery in certain circumstances. The use of complex reaction schemes in numerical modeling remarkably enhances the prediction of experimental reservoir data.

Keywords: numerical reservoir simulation; in situ upgrading; heavy crude oil recovery; steam injection technologies

check for updates

Academic Editors: Renbao Zhao and Xuyang Guo

Received: 16 September 2025
Revised: 21 October 2025
Accepted: 24 October 2025
Published: 27 October 2025

Citation: Kwofie, M.; Félix, G.; Tirado, A.; Varfolomeev, M.A.; Ancheyta, J. Advances in Numerical Reservoir Simulation for In Situ Upgrading of Heavy Oil via Steam-Based Technologies. *Energies* **2025**, *18*, 5639. https://doi.org/10.3390/en18215639

Copyright: © 2025 by the authors. Licensee MDPI, Basel, Switzerland. This article is an open access article distributed under the terms and conditions of the Creative Commons Attribution (CC BY) license (https://creativecommons.org/licenses/by/4.0/).

1. Introduction

The increasing demand for energy sources and the depletion of light oil reserves have caused researchers to consider alternative supplies. Unconventional hydrocarbon reservoirs are a possible alternative to meet the demand for fuel supply. These reservoirs

contain highly viscous oils, hindering their mobility and extraction; thus, in situ upgrading processes are needed for these types of hydrocarbons. Nevertheless, upgrading of heavy crude oils and bitumen is not an easy task since the elevated number of high-molecular-weight compounds, such as asphaltenes and resins, makes it difficult to break into lower-molecular-weight fractions [1–4]. This complexity is compounded when modeling the aquathermolysis reaction, as it involves a complex network of simultaneous thermal, catalytic, and hydrogen-donating reactions between oil, water, and reservoir rock minerals, all under extreme conditions that are difficult to observe and quantify.

Enhanced oil recovery methods are the most applied to the in situ upgrading of heavy crude oils and bitumen since they achieve higher recovery rates of these hydrocarbons. Among these, thermal methods are preferred because the application of heat considerably reduces the viscosity and increases the mobility of heavy and extra-heavy oils [5–9]. Steam injection technologies are employed worldwide because of their proven effectiveness in reducing the viscosity of heavy hydrocarbons. Usually, three types of steam injection technologies are applied to in situ heavy crude oil upgrading: cyclic steam stimulation (CSS), steam flooding (SF), and steam-assisted gravity drainage (SAGD). The operational principles and specific applications of these three key technologies are detailed in the following subsections.

Regarding CSS, which is the most used technology for steam injection in situ recovery of heavy oil, three main steps are considered in one cycle: (1) steam injection, where the steam is injected into the reservoir for several weeks, (2) soaking, where the well is closed to leave the steam and heavy oil to react for several days, transferring the heat from the steam to neighboring layers, and (3) oil production, where the well is open to recover the lower viscosity oil (several weeks or months). Cyclic steam injection is normally limited to recovering about 25% of the original oil-in-place. This ceiling exists because the process becomes less efficient with each cycle, as the growing steam zone leads to greater heat losses to the cap rock [5–8,10–15].

The SF technology is the next stage of CSS since steam is continuously injected into the reservoir to heat the heavy crude oil, enhancing its viscosity and causing the oil and condensed water to flow to the producer well. This technology type suits reservoirs with porosity, oil saturation, and thickness higher than 20%, 0.5, and 10 m, respectively. While SF can achieve high recovery factors and consistent production, it is a resource-intensive method. It is ideally applied to large, homogeneous reservoirs with good inter-well communication and requires substantial capital for infrastructure. Operators must also manage inherent challenges, such as steam channeling and heat losses to maintain efficiency.

Unlike CSS, which uses a single well for cyclic injection and production, both SF and SAGD employ multiple wells. However, while the former typically uses vertical injection and production wells, SAGD utilizes a unique well pair consisting of two closely spaced horizontal wells, with steam injection in the upper well and production in the lower well, placed at the bottom of the reservoir. In this technology, the continuous injection of steam provokes steam chamber growth. When the steam reaches the boundaries of the steam chambers, it exchanges heat with the surrounding heavy oil to reduce its viscosity and flow to the production well. SAGD generates more water-in-oil emulsions than SF technology, increasing the interaction of water with the principal reagents in heavy oil [6,10–13].

These steam injection technologies have gained the increased interest of researchers because their recovery factor can be enhanced by the addition of catalysts. Nonetheless, the different catalysts (water-soluble, oil-soluble, dispersed, mineral, ionic liquids) are only applied to a bench-scale stage, showing adequate results in improving the mobility and recovery of heavy oil [14–16]. Scaling up this type of technology requires a complete understanding of the physical and chemical phenomena to design and optimize the operating

conditions and technical issues, such as the methodology of injection, optimal parameters, selection of catalyst, etc. The best way to obtain more appropriate steam injection technology is by applying physical and numerical simulation of reservoirs using different conditions to find an optimal strategy to enhance the oil recovery factor in fields [13,15,17].

The complexity of the chemical reactions involved during the in situ upgrading of heavy oil has led to the development of complex kinetic models. Several laboratory-scale studies [18–22] have focused on enhancing aquathermolysis reactions by combining steam with catalyst injection, resulting in kinetic models tailored for these specific conditions. However, a significant gap exists as these models are often not developed or validated under full reservoir conditions. Consequently, numerical reservoir simulation becomes an indispensable tool for describing the coupled kinetic and thermodynamic phenomena occurring during in situ steam injection. The simulation of steam-based Enhanced Oil Recovery (EOR) processes, such as SAGD, is inherently a formidable task. Its accuracy is governed by a correct representation of multiphase flow, heat transfer, and chemical reactions. Parametric studies have consistently highlighted that the success of these models is highly sensitive to key inputs, with the accuracy of the simulated thermal front being paramount for predicting oil production rates and recovery factors [23–25]. A critical factor controlling the propagation of this thermal front is the accurate representation of temperature-dependent rock thermal properties, such as thermal conductivity and heat capacity [26,27]. To effectively understand the dynamics of heat transport in geological formations, it is essential to consider the concept of spatial heterogeneity. This term refers to the intricate, non-uniform, and often unpredictable variations in geological properties across different areas. Such complexity can significantly influence the behavior of streams, compelling them to follow preferential pathways. As a result, these streams might become trapped in zones characterized by high permeability while completely bypassing regions with low permeability. This selective flow alters the movement of steam and has profound implications for heat transport within the geological system. Thus, it is crucial to conduct a thorough analysis and evaluation of the thermal properties of rocks. By accurately determining these values, one can predict the pathways of heat and assess their consequent effects on the surrounding environment [28–30]. The numerical representation of these properties is not trivial, as they significantly influence the shape and growth of the steam chamber, thereby directly impacting oil production forecasts [31,32].

Furthermore, the expansion of the reservoir and caprock due to heating introduces critical geomechanical considerations. The phenomenon of thermal expansion can induce significant stresses, making its inclusion essential for assessing caprock integrity and ensuring the safe operation of an SAGD process [33]. Sequentially coupled thermal–hydraulic–mechanical (THM) simulations have demonstrated that geomechanical deformations have a substantial impact on oil production and steam chamber growth. These deformations involve shear failures that form high-permeability planes, allowing steam to bypass shale barriers. This process leads to a significantly more accurate prediction of both hydrocarbon production and surface heave. The underlying mechanism is the differential propagation speed between the pressure and temperature fronts, which alters the stress paths [34]. Despite the importance of these physical phenomena, many numerical simulation studies resort to simplifications. Significant factors such as chemical reactions described by robust kinetic models, the adsorption of heavy molecules on nanoparticles in catalytic processes, or the reduction in catalyst activity are often simplified or omitted. This is frequently due to the computational intensity required to integrate such details with the already complex representation of formation and fluid properties [35–38].

In situ steam injection processes commonly employ catalysts that are water- or oil-soluble, dispersed, or mineral-based, typically formulated with transition metals such

as nickel, molybdenum, iron, or copper. These materials show strong catalytic activity at the beginning of operation, but tend to lose effectiveness with repeated cycles. This performance can be attributed to the fact that part of the catalyst becomes retained in the rock matrix, reducing overall catalytic efficiency and, consequently, the recovery factor. Thus, a comprehensive study and representation of catalyst dispersion stability, migration, and adsorption within the reservoir are necessary to design and optimize efficient injection protocols and accurate numerical calculations [39,40].

Different approaches have been considered during the numerical reservoir simulation for the aquathermolysis of heavy crude oil, considering diverse parameters that affect the results obtained. Therefore, this work performs an exhaustive analysis and discussion of the various approaches reported in the literature for numerical reservoir simulation for the in situ upgrading of heavy crude oil to achieve a precise understanding of the advances and challenges addressed in the production of unconventional oil reserves. Specifically, this review focuses on the critical gap between bench-scale catalytic promise and field-scale application. The existing kinetic models and numerical simulation frameworks that integrate catalytic effects, with a particular emphasis on how they handle complex phenomena, such as catalyst adsorption, deactivation, and transport within the reservoir, are systematically categorized and evaluated. By synthesizing these disparate approaches, this work aims to provide a clear roadmap for developing more robust and predictive simulation tools, which is an essential step toward the successful design and implementation of catalytic steam injection processes in the field.

2. Numerical Simulations for Aquathermolysis of Heavy Crude Oil

Numerical simulation offers a pathway to optimize in situ aquathermolysis, a promising method for recovering heavy oil by using heat and water to break down complex molecules. Simulations attempt to replicate this process by integrating kinetic models of chemical reactions (e.g., hydrolysis, thermal cracking) with reservoir-scale models of fluid flow and heat transfer using tools such as CMG STARS (Steam Thermal Advanced Recovery Simulator) or UTCHEM [41,42]. Despite their potential, these simulations face critical limitations that impact their predictive reliability. First, the computational cost is prohibitive; resolving the fine-scale geochemical interactions across a full reservoir model with finite element or volume methods demands exceptional resources, often limiting the scope or detail of the study. Second, models are plagued by significant uncertainties, particularly in the kinetic parameters of aquathermolysis reactions and the evolving fluid properties at extreme conditions [43–45].

Commercial simulators address this complexity by solving coupled equations for mass, energy, and momentum conservation, incorporating reactive transport through kinetic reaction networks. However, their forecasting reliability is critically influenced by several uncertainties. Key among these are the kinetic parameters for aquathermolysis reactions, which are often extrapolated from lab-scale experiments, and the heterogeneous distribution of reservoir permeability, which controls the delivery of heat and reactants. Furthermore, uncertainties in operational parameters, such as downhole steam quality, directly impact the predicted temperature field and reaction rates. Consequently, a model tuned to historical data may fit the past but remains unreliable for forecasting future performance or extrapolating to new field applications due to these inherent limitations. Therefore, a critical challenge in the field is to develop efficient and robust simulation frameworks that explicitly account for these limitations to provide more trustworthy forecasts for field applications such as the development of hybrid models (coupling physics-based simulations with machine learning surrogates), advanced upscaling methods to capture

sub-grid geochemical effects, and the integration of rigorous uncertainty quantification frameworks [30,46].

All these parameters in the model can be modified to increase the degree of agreement between experimental behavior and simulation results. Furthermore, a sensitivity analysis can be performed to evaluate the effects of important parameters (such as temperature, pressure, and water-to-oil ratio) on the production results. These numerical simulation models can be validated against experimental data or field observations of steam injection processes. Table 1 summarizes several works that have applied the numerical reservoir simulation to predict the recovery of different heavy crude oils using steam injection technologies. All these literature reports are described and analyzed in the following sections.

2.1. Without Aquathermolysis Reactions

Ito and Suzuki [47] conducted a simulation study employing the Hangingstone tar sands reservoir to project recovery rates and elucidate the oil recovery mechanism during the SAGD process. Initially, the data are selected from three different wells utilizing gamma-ray logs to ascertain shale content at intervals of 0.5 m within a 30 m formation. For the reservoir-scale model, a grid was constructed consisting of $33 \times 3 \times 17$ cells (with dimensions of 50 m, 500 m, and 30 m in the x, y, and z directions, respectively), employing the STARS software of CMG. The injection and production wells were positioned 5.5 m above the base of the formation, with a separation of 5 m between them. The numerical model was subjected to constraints: a maximum bottom hole pressure of 5000 kPa and a maximum oil production rate of 40 m^3/day for the producer well. The injected steam (quality of 98%) was introduced over a period of 6.1 years. However, a significant limitation of this model was its treatment of the system as non-reactive; by ignoring the complex chemical reactions between steam and the reservoir formation, such models are known to risk overestimating the ultimate recovery factor.

Table 1. Reservoir properties reported in the literature for the numerical simulation during steam injection upgrading of heavy oil.

Property	Ito and Suzuki [47]	Gillis et al. [48]	Sasaki et al. [49]	Ovalles and Rodriguez [50]	Perez-Perez et al. [51]	Ibatullin et al. [36]	Kapadia et al. [52]	Ayache et al. [53]	Zhang et al. [16]	Yuan et al. [54]	Wang et al. [55]	Nguyen et al. [56]	Hassanzadeh et al. [38]	Huang et al. [17]	Bueno et al. [37]	Yang et al. [57]
Reservoir	Hangingstone			Hamaca	Athabasca bitumen		Athabasca bitumen	Athabasca bitumen								Athabasca bitumen
Top depth (m)					300	300	320	300	110	750				124		
Total dimensions (m)																
x	50	1.5		10		30		420	0.6	0.5	0.01	1	30		91.44	50
y	500	2		1		50		150	0.6	0.6	0.002	50	101		5.12	1.5
z	30	24		10		800		18	0.35	0.5	0.002	1	1		778.76	20
Horizontal permeability (mD)		5000	1.42×10^5		3000	7000	2424	10,000		1860	2450	3600	5000	2656	1000	4000
Vertical permeability (mD)		2500			1000	3500	485	3500				1800				3000
Porosity, fraction		0.3	0.38	0.33	0.3	0.33		0.37		0.2511		0.33	0.3	0.3	0.26	0.33
Initial pressure (kPa)			101.3	8000	1000		2600	2900		4000		2000	1300	2550		1500
Initial temperature (°C)			20	53	10	11	10	17		37		11	7	13		13
Rock-heat capacity (J/m^3-°C)			1.99×10^6			2.63×10^6	2.60×10^6	2.31×10^6		2.60×10^6	2.58×10^6		1.20×10^6			2.60×10^5
Rock-thermal conductivity (J/m-s-°C)		1.16	1.17			2.5	7.64	2.75		7.64	1.89		7.22			7.64
Oil density (g/cm^3)			0.998			1.013				1.001		1.0129				
Oil gravity (°API)					8	8.2		10								
Oil viscosity (cP)					1.7×10^6	1.5×10^6		3.8×10^6				654.228		35,438		
Pay zone (m)				27.4	40	30	28			30			30			
Initial oil saturation		1		0.87	0.8	0.8	0.64	0.78		0.64	0.7–0.82	0.81	0.85	0.7	0.8	0.75
Initial water saturation		0		0.13	0.2	0.2	0.34	0.22		0.36	0.3–0.18	0.19	0.15	0.3	0.2	0.25
Maximum BHP (kPa)	5000					3350	1000–5000					2656				2730
Maximum production rate (m^3/d)	40															
Injection rate (m^3/d)				397.5					400	192	250	191				
Steam quality (%)				75			90		90		70	95				90

Gillis et al. [48] presented a numerical analysis based on theoretical principles on the historical gas production (H_2S, CO_2, and CH_4) during SAGD using data from the experiment conducted by Hyne and Clark [58]. Through these experimental findings, equilibrium values (K) were established for CH_4 and H_2S within bitumen, employing a general equilibrium correlation (Equation (1)) and sensitivity analysis, which exhibited a favorable agreement with experimental observations. Additionally, the solubility of gas in water was determined by employing a series of correlations incorporating Henry's constant (k_H), pressure, and the ratio of mole fractions, as follows:

$$K = \left(\frac{a}{P}\right) exp\left(\frac{b}{T-c}\right) \tag{1}$$

$$k_H = \frac{y_g P \phi_g}{\gamma_g x_g} exp \int_{p*}^{P} \frac{v dP}{RT} \tag{2}$$

$$K = \frac{k_H}{P} \tag{3}$$

$$K = \frac{y_g}{x_g} \tag{4}$$

The thermal simulator developed by CMG, known as STARS, was employed for the numerical model, where a well pair spanning 500 m was integrated, with the production well situated at the base of the formation and the injection well positioned 3 m above it. This work directly addressed the chemical limitations of previous models [47], yet its own methodology, which relied heavily on equilibrium assumptions, may not fully capture the kinetic limitations and transient nature of these reactions under dynamic reservoir conditions. The horizontal permeability of the bitumen, deduced from core data, exhibited an average value of 5000 mD in the vicinity of the well pair, gradually reducing to 1000 mD near the upper limits of the reservoir. Vertical permeability was established at half the horizontal value, while the porosity fluctuated between 0.3 and 0.35, depending on the quality of the sand. The grid utilized within the model consisted of blocks measuring 1.5 m in the x-direction, 2.0 m in the y-direction, and 24 blocks of 1 m in the z-direction. This selection was made to minimize errors associated with discretization and numerical dispersion.

Sasaki et al. [49] and Nie et al. [59] conducted research focused on the numerical well history matching experimental data, specifically oil production and steam chamber temperature contours. For this study, a scaled reservoir model was designed, which has several two-dimensional visual plates with acrylic resin sidewalls (20 mm thick) to simulate a vertical section of the heavy oil reservoir. While this setup provided invaluable direct visual observation of the process, the 2D nature of the model and the use of acrylic materials introduce geometric and thermal simplifications that limit its direct applicability to a full 3D, field-scale reservoir. With this model, the duration needed to establish initial communication between the steam injection and production wells, known as steam breakthrough time, was investigated, and the phenomena associated with the ascending steam chamber were explored. The reservoir-scale model tests maintained a constant steam (quality of 100%) injection absolute pressure of 121.3 kPa at a temperature of 105 °C. These experiments were conducted using a Cartesian grid system comprising 15 × 3 × 15 cells in the x, y, and z directions, respectively. The porosity of the reservoir was 0.38 with an average permeability of 1.42×10^5 mD, a thermal conductivity of 1.17 J/m-s-°C, and a volumetric heat capacity of 1.99×10^6 J/m^3-°C. The thermal properties of the resin material used to fabricate the model were measured, obtaining a thermal conductivity of 0.22 J/m-s-°C and a volumetric heat capacity of 1.67×10^6 J/m^3-°C.

2.2. With Aquathermolysis Reactions

A variety of research works have presented both straightforward and complex reaction schemes (as illustrated in Figure 1) to thoroughly explore the aquathermolysis reaction within the framework of numerical simulation calculations. These schemes aim to enhance our understanding of the intricate processes involved in aquathermolysis, shedding light on the mechanisms performing in this chemical reaction.

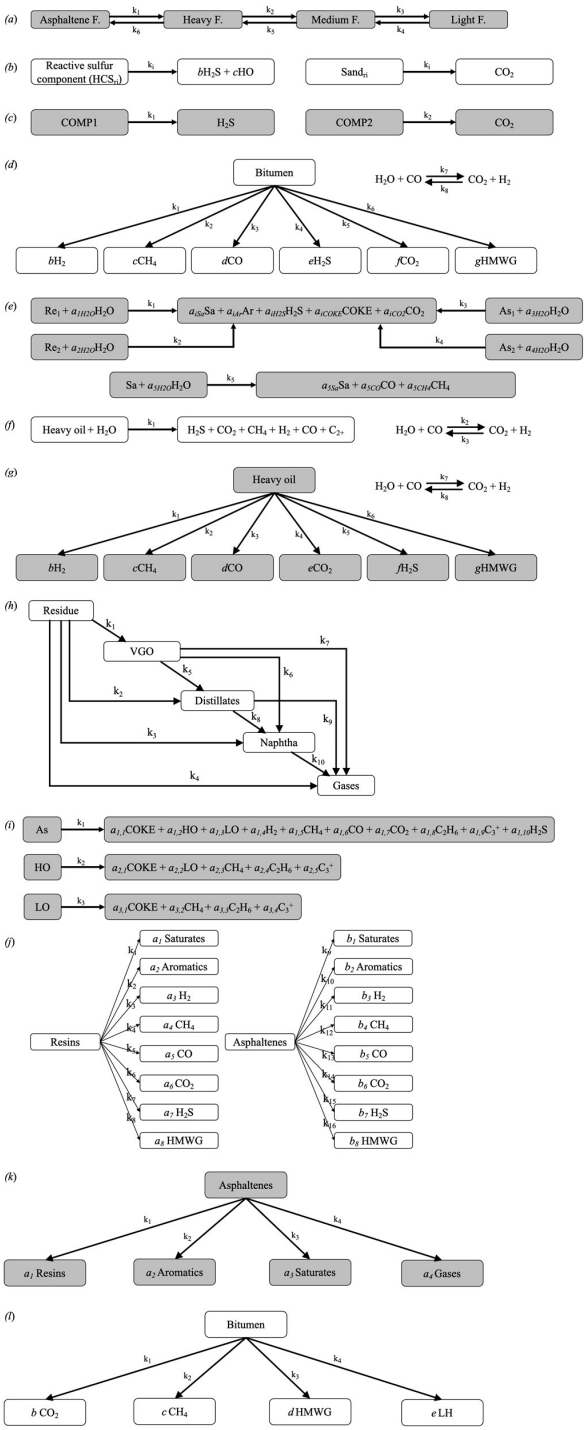

Figure 1. Reaction schemes reported in the literature to represent the aquathermolysis reactions for the numerical simulation during steam injection upgrading of heavy oil. (**a**) Ovalles et al. [60], (**b**) Perez-Perez et al. [51], (**c**) Ibatullin et al. [36], (**d**) Kapadia et al. [52], (**e**) Ayache et al. [35], (**f**) Zhang et al. [16], (**g**) Yuan et al. [54], (**h**) Nguyen et al. [56], (**i**) Hassanzadeh et al. [38] and Yang et al. [57], (**j**) Huang et al. [17], (**k**) Bueno et al. [37], and (**l**) Yang et al. [57].

Ovalles et al. [60] developed a numerical reservoir model utilizing Orinoco Belt Hamaca heavy crude oil and a hydrogen donor (tetralin) to predict the distributions of liquid phase products during downstream steam injection upgrading. The initial procedure involved blending methane with a homogeneous mixture of Hamaca crude oil and tetralin to generate a continuous flow of live crude oil. Subsequently, this amalgam was introduced into the reactor alongside the water in a mass ratio of 10:1:1:1 (sand, crude oil, water, and tetralin). All the experiments were performed in a continuous pilot plant at different operating conditions: temperatures of 280–315 °C, pressure of 11,700 kPa, and residence times of 16, 32, and 64 h. Additional tests were performed to determine the reaction order of tetralin at 300 °C in a batch reactor. With these experimental data, a kinetic model (Figure 1a) was developed based on four pseudocomponents with different distillation ranges: asphaltenes, a light fraction (room temperature to 210 °C), a medium fraction (210–340 °C), and a heavy fraction (340 °C+). In the supposed reaction scheme, these lumps react from higher-molecular-weight fractions into lighter molecules by cracking reactions. Additionally, the corresponding reversible reactions were considered to obtain the following reaction pathways:

$$\text{Asphaltene F} + \text{Tetralin} \xrightarrow{k_1} \text{Heavy F} + \text{Naphthalene} \quad (5)$$

$$\text{Heavy F} + \text{Tetralin} \xrightarrow{k_2} \text{Medium F} + \text{Naphtalene} \quad (6)$$

$$\text{Medium F} + \text{Tetralin} \xrightarrow{k_3} \text{Light F} + \text{Naphtalene} \quad (7)$$

$$\text{Light F} \xrightarrow{k_4} \text{Medium F} \quad (8)$$

$$\text{Medium F} \xrightarrow{k_5} \text{Heavy F} \quad (9)$$

$$\text{Heavy F} \xrightarrow{k_6} \text{Asphaltene F} \quad (10)$$

Once the kinetic parameters were estimated, a commercial simulator (STARS from CMG) was used to perform the numerical model simulations at bench and reservoir scales. Initially, the numerical simulation was performed at the bench scale to corroborate that the obtained model can predict properly the experimental data. In this first model, the following parameters were employed: cylindrical grid ($4 \times 1 \times 4$), initial temperature of 280–315 °C, initial pressure of 11,032 kPa, permeability of 11,500 mD, and oil saturation of 0.666 (0.333 water saturation). Once the numerical model simulation at the pilot plant scale was corroborated, a reservoir scale application was carried out. The Hamaca reservoir was simulated at CSS conditions, where a blend of steam and tetralin (1:1, 75% quality steam) was injected into the well (397.5 m^3/d) for 20 days, followed by a soaking period of 10 days. Here, a $10 \times 1 \times 10$ cylindrical grid, permeability of 12,000 mD, pay zone of 27.4 m, porosity of 32.5%, oil saturation of 0.87, an initial temperature of 58.3 °C, and pressure of 8000 kPa were employed for the reservoir simulation. For the reservoir numerical simulation scale, two approaches were used with and without the aquathermolysis reactions to compare the effect of kinetic models on the numerical model predictions.

Another numerical reservoir simulation model was developed by Perez-Perez et al. [51] using the experimental data for the aquathermolysis reaction of Athabasca bitumen reported by Hyne et al. [58,61] for the H_2S and by Hyne and Tyrer [62], Hyne and Clark [63], and Clark et al. [64] for the CO_2. Different tests were conducted at temperatures of 180–240 °C and a reaction time of 90 days in a batch reactor. Firstly, the authors developed a kinetic model (Figure 1b) with the obtained experimental data based on a set of kinetic equations to forecast the production of H_2S and CO_2 from inorganic sources and organosulfur oil molecules (within the bitumen), respectively. Precursors of H_2S and CO_2, reactive

sulfur species of asphaltenes and resins (HCSr) in bitumen, and reactive sand (Sand) are grouped in the suggested reaction scheme. Since not all organosulfur compounds convert under the same circumstances, this approach presents a collection of parallel reactions as a function of temperature intervals. The corresponding reactions were considered to obtain the following reaction pathways:

170 °C < T < 190 °C:

$$HCS_{r(1)} \xrightarrow{k_1} bH_2S + cHO \quad (11)$$

$$Sand_{r(1)} \xrightarrow{k_1} CO_2 \quad (12)$$

190 °C < T < 210 °C:

$$HCS_{r(1)} \xrightarrow{k_1} bH_2S + cHO \quad (13)$$

$$HCS_{r(2)} \xrightarrow{k_2} bH_2S + cHO \quad (14)$$

$$Sand_{r(1)} \xrightarrow{k_1} CO_2 \quad (15)$$

$$Sand_{r(2)} \xrightarrow{k_2} CO_2 \quad (16)$$

210 °C < T < 230 °C:

$$HCS_{r(1)} \xrightarrow{k_1} bH_2S + cHO \quad (17)$$

$$HCS_{r(2)} \xrightarrow{k_2} bH_2S + cHO \quad (18)$$

$$HCS_{r(3)} \xrightarrow{k_3} bH_2S + cHO \quad (19)$$

$$Sand_{r(1)} \xrightarrow{k_1} CO_2 \quad (20)$$

$$Sand_{r(2)} \xrightarrow{k_2} CO_2 \quad (21)$$

$$Sand_{r(3)} \xrightarrow{k_3} CO_2 \quad (22)$$

230 °C < T < 250 °C:

$$HCS_{r(1)} \xrightarrow{k_1} bH_2S + cHO \quad (23)$$

$$HCS_{r(2)} \xrightarrow{k_2} bH_2S + cHO \quad (24)$$

$$HCS_{r(3)} \xrightarrow{k_3} bH_2S + cHO \quad (25)$$

$$HCS_{r(4)} \xrightarrow{k_4} bH_2S + cHO \quad (26)$$

$$Sand_{r(1)} \xrightarrow{k_1} CO_2 \quad (27)$$

$$Sand_{r(2)} \xrightarrow{k_2} CO_2 \quad (28)$$

$$Sand_{r(3)} \xrightarrow{k_3} CO_2 \quad (29)$$

$$Sand_{r(4)} \xrightarrow{k_4} CO_2 \quad (30)$$

After estimating the kinetic parameters, the thermal simulator STARS (2009 release) developed in CMG was used to create a numerical reservoir model that represents the production of the Athabasca oil sand and these gases in the oilfield. The reservoir has a pay-zone thickness of 40 m, a depth of 300 m, 10 °C in temperature, and an initial saturation of oil and water of 0.8 and 0.2, respectively. The reservoir deposit is made up entirely of sand; no particular heterogeneities were mentioned. The absolute permeability is 1000 mD

for the vertical direction and 3000 mD for the horizontal direction. The porosity is always set at thirty percent. Following the simulation, the outcomes were examined.

Ibatullin et al. [36] formulated a practical engineering methodology to simulate and predict the production of H_2S and CO_2 during the thermal recovery process, incorporating chemical reactions into the pre-existing PVT model of bitumen. This approach employs a simplified kinetic model (Figure 1c) where all potential reaction pathways are consolidated into two primary reactions: COMP1, treated as a single pseudocomponent responsible for H_2S production, and COMP2, treated as a single pseudocomponent responsible for CO_2 production. The reaction scheme is expressed through the following equations:

$$r_1 = \mathrm{k_1(T)[COMP1][H_2O]} \tag{31}$$

$$r_2 = \mathrm{k_2(T)[COMP2][H_2O]} \tag{32}$$

$$\mathrm{k_1(T)} = A_1 exp\left(\frac{-E_{A_1}}{RT}\right) \tag{33}$$

$$\mathrm{k_2(T)} = A_2 exp\left(\frac{-E_{A_2}}{RT}\right) \tag{34}$$

For the numerical simulations, a reservoir-scale model (using the CMG software) was implemented with a grid consisting of 30 × 50 × 800 m (each block in the grid of 1 m, 800 m, and 1 m for x, y, and z directions, respectively). Within this model, a well pair spanning 500 m was established, with a vertical separation of 5 m between them, being the producer positioned 1.5 m above the reservoir base. After three months of preheating, the wells were transitioned to the normal SAGD operating regime, with a maximum bottom hole pressure (BHP) of 3350 kPa, a saturated steam temperature of 240 °C, and a steam quality of 90%. Finally, the production period was set for 20 years.

Kapadia et al. [52] created a numerical reservoir simulation model using Athabasca oil sands to predict the gas phase product distributions during a typical SAGD operation. A simple kinetic model (Figure 1d) that considers Bitumen as a single pseudocomponent in the liquid phase, which produces gases including H_2, CO_2, CO, H_2S, CH_4, and HMWG (high-molecular-weight gases) through cracking reactions. Some of these gases can afterward react by the water-gas shift reaction. This reaction scheme is represented by the following equations:

$$\text{Bitumen} \rightarrow 230.6413\ \mathrm{H_2} \tag{35}$$

$$\text{Bitumen} \rightarrow 28.9822\ \mathrm{CH_4} \tag{36}$$

$$\text{Bitumen} \rightarrow 16.5993\ \mathrm{CO} \tag{37}$$

$$\text{Bitumen} \rightarrow 10.5647\ \mathrm{CO_2} \tag{38}$$

$$\text{Bitumen} \rightarrow 13.6423\ \mathrm{H_2S} \tag{39}$$

$$\text{Bitumen} \rightarrow 11.2268\ \text{HMWG} \tag{40}$$

$$\mathrm{CO + H_2O \rightleftarrows CO_2 + H_2} \tag{41}$$

For the reservoir-scale model, which is performed using the CMG software STARS (2010 release), 10,620 grid blocks were employed with different sizes: when the grids are less than 10 m away from the wells, a value of 0.35 m is applied. However, for grids beyond this value, 0.67 m is used. Each block has a vertical height of 0.46 m. With a depth of 320 m, the top of the oil column is around 28 m thick. A high-quality steam (90%) is injected, varying the bottom-hole pressure in a range of 1000–5000 kPa to study the influence of steam temperature on the production of hydrogen sulfide. The area surrounding the wells

is preheated for three months before beginning SAGD operation using line heaters in horizontal well locations. Data on the relative permeability of water, oil, and liquid–gas were gathered from an SAGD pilot history match in an Athabasca oil sands reservoir [65]. The aqueous phase solubility of CH_4, CO_2, and H_2S is characterized by K-values, as reported elsewhere [52].

Ayache et al. [35] reported a numerical reservoir simulation model for the SAGD technology of Athabasca bitumen with experimental data obtained by Lamoureux-Var et al. [66–68]. Different tests were performed at temperatures of 240–320 °C, pressure of 10,000 kPa, and reaction times of 24 and 203 h in a closed gold tube. The authors presented a kinetic model (Figure 1e) based on the chemical interactions between steam and oil components to determine H_2S levels and the change in the composition of SARA (Sa, Ar, Re, and As) fractions within oil as follows:

$$\mathrm{Re_1} + a_{1\mathrm{H_2O}}\mathrm{H_2O} \rightarrow a_{1\mathrm{Sa}}\mathrm{Sa} + a_{1\mathrm{Ar}}\mathrm{Ar} + a_{1\mathrm{H_2S}}\mathrm{H_2S} + a_{1\mathrm{COKE}}\mathrm{COKE} + a_{1\mathrm{CO_2}}\mathrm{CO_2} \quad (42)$$

$$\mathrm{Re_2} + a_{2\mathrm{H_2O}}\mathrm{H_2O} \rightarrow a_{2\mathrm{Sa}}\mathrm{Sa} + a_{2\mathrm{Ar}}\mathrm{Ar} + a_{2\mathrm{H_2S}}\mathrm{H_2S} + a_{2\mathrm{COKE}}\mathrm{COKE} + a_{2\mathrm{CO_2}}\mathrm{CO_2} \quad (43)$$

$$\mathrm{As_1} + a_{3\mathrm{H_2O}}\mathrm{H_2O} \rightarrow a_{3\mathrm{Sa}}\mathrm{Sa} + a_{3\mathrm{Ar}}\mathrm{Ar} + a_{3\mathrm{H_2S}}\mathrm{H_2S} + a_{3\mathrm{COKE}}\mathrm{COKE} + a_{3\mathrm{CO_2}}\mathrm{CO_2} \quad (44)$$

$$\mathrm{As_2} + a_{4\mathrm{H_2O}}\mathrm{H_2O} \rightarrow a_{4\mathrm{Sa}}\mathrm{Sa} + a_{4\mathrm{Ar}}\mathrm{Ar} + a_{4\mathrm{H_2S}}\mathrm{H_2S} + a_{4\mathrm{COKE}}\mathrm{COKE} + a_{4\mathrm{CO_2}}\mathrm{CO_2} \quad (45)$$

$$\mathrm{Sa} + a_{5\mathrm{H_2O}}\mathrm{H_2O} \rightarrow a_{5\mathrm{Sa}}\mathrm{Sa} + a_{5\mathrm{CO_2}}\mathrm{CO_2} + a_{5\mathrm{CH_4}}\mathrm{CH_4} \quad (46)$$

Initially, in a private reservoir simulation software, a 0D reservoir model of one cell (figuring the gold tube) surrounded by cells representing the oven was used by applying a Peng-Robinson equation of state based on the molar mass of components to calibrate the thermal-kinetic model of aquathermolysis experiments. Subsequently, the 2D reservoir model was employed to simulate the reservoir scale based on a rectangular cross-section (x = 420 m, y = 150 m, and z = 18 m) with uniform permeability and porosity. A grid with 3375 cells (1 × 75 × 25) was applied, where the horizontal wells are situated halfway in the y-axis, separated by 6 m in the z-axis, and with a length of 420 m in the x-axis. The top of the reservoir is located at 300 m under the surface with an initial pressure of 2900 kPa. A preheating period of 4 months for the wells was considered to mobilize the bitumen. Some limits are subject to the flow rate of the producer and injection wells based on their temperatures. The producer flow rate is diminished if the difference between the injection and production temperatures is equal to or lower than 20 °C. This will allow migrating the steam chamber from the producer, lowering the temperature, and increasing the volume of liquid around the well. In the same way, the producer flow rate is raised if the difference between injection and production temperatures is equal to or above 35 °C.

Zhang et al. [16] conducted a study using a geological model that integrates the core-catalyzed aquathermolysis to simulate the extraction process in the SAGD method. A general kinetic model (Figure 1f, Equations (47) and (48)) was employed for the numerical reservoir simulation, contemplating heavy oil as a pseudo-component and incorporating eight reactions (considering also the water-gas shift reaction) as described by Kapadia et al. [69]:

$$\text{Heavy oil} + \mathrm{H_2O} \rightarrow \mathrm{H_2S} + \mathrm{CO_2} + \mathrm{CH_4} + \mathrm{H_2} + \mathrm{CO} + \mathrm{C_{2+}} \quad (47)$$

$$\mathrm{CO} + \mathrm{H_2O} \rightleftarrows \mathrm{CO_2} + \mathrm{H_2} \quad (48)$$

For the reservoir simulation, the model comprised 66,960,000 grid blocks (800 × 270 × 310). The reservoir had a thickness of 110 m, with grid steps of 0.6 m in both the x and y directions, each grid block had a height of 0.35 m in the z-direction (vertical direction). The steam

injection parameters for the simulation were directly derived from actual production data, with 90% quality steam injected at the wellhead at a flow rate of 400 m^3/day and a temperature of 240 °C (3350 kPa).

Yuan et al. [54] utilized geological parameters from the Xing VI block to develop a reservoir numerical model that incorporates aquathermolysis reactions, which was implemented in CMG-STARS. A simple reaction scheme (Figure 1g) with several parallel reactions was employed, which is documented in previous studies [16,17,69]. Within this model, heavy oil in the oil phase is decomposed into acid (H_2S, CO, and CO_2) and organic (H_2, CH_4, and HMWG) gases during the aquathermolysis, together with the water-gas shift reaction. Reaction equations were derived based on the principles of mass conservation to describe the behavior of these components in the system.

$$0.1667 \text{ Heavy oil} \rightarrow 54.0783 \ H_2 \quad (49)$$

$$0.1667 \text{ Heavy oil} \rightarrow 6.7969 \ CH_4 \quad (50)$$

$$0.1667 \text{ Heavy oil} \rightarrow 3.8922 \ CO \quad (51)$$

$$0.1667 \text{ Heavy oil} \rightarrow 2.4772 \ CO_2 \quad (52)$$

$$0.1667 \text{ Heavy oil} \rightarrow 3.1990 \ H_2S \quad (53)$$

$$0.1667 \text{ Heavy oil} \rightarrow 2.6327 \text{ HMWG} \quad (54)$$

$$CO + H_20 \rightleftarrows H_2 + CO_2 \quad (55)$$

A reservoir model consisting of 221 × 1 × 60 grid blocks (with a size of 0.5 m within the first 10 m around the well pair, extending to 0.6 m beyond this radius, and vertically 0.5 m) was employed, with the top boundary located at a depth of 750 m. Each horizontal well extended 300 m within the reservoir with a pay thickness of 30 m. The production well was situated 5 m above the reservoir bottom, with a 5 m separation from the injection one. The developed numerical model was validated using data from a self-manufactured device to simulate the whole SAGD process (steam injection, reservoir simulation, back-pressure, and data-acquiring systems).

Wang et al. [55] conducted a numerical study contemplating a kinetic model for the H_2S generation during the CSS of Bohai Bay heavy oil. Various tests were carried out in a closed autoclave reactor at temperatures between 270 and 300 °C with reaction times of 12 and 48 h. The kinetic parameters were calculated using a reaction scheme (Figure 1d) reported by Kapadia et al. [70]. After this, continuous experimental tests were performed in a one-dimensional reactor filled with silica sand. Water and heavy oil were injected into the sand pack reactor using a pump, and the porosity, permeability, and initial oil saturation were measured at 56.8%, 2748 mD, and 85.4%, respectively. Distilled water was heated to 300 °C by a steam generator, and near 100% quality steam was injected into the model at a rate of 14.4 m^3/day until the reservoir pressure reached 1000 kPa. Each cycle of steam injection and soaking lasted a total of 2 h. The CMG-STARS software was employed to create a numerical model for simulating H_2S generation during a one-dimensional CSS experiment. For simulations, a grid configuration of 48 × 19 × 19 (17,328 grids) with a size of 0.01 × 0.002 × 0.002 m (in x, y, and z directions) was used.

2.3. With Aquathermolysis Reactions and Catalyst Injection

Some of these steam injection technologies have applied catalysts to improve the recovery factor and the quality of bitumen and heavy crude oils [71–73]. Nguyen et al. [56] investigated a numerical reservoir model of bitumen/heavy oil upgrading by injecting steam along with a mixture of hydrogen, catalyst (ammonium heptamolybdate, ammonium

metatungstate, nickel acetate, and ammonium sulfide), and vacuum residue to improve the quality of the produced oil by transforming heavy oil components into lighter oil components. A five-lump kinetic model (Figure 1h) proposed by Sanchez et al. [74] is employed in the numerical reservoir simulation, which considers residue (R, 550 °C+), vacuum gas oil (VGO, 343–550 °C), distillates (D, 216–343 °C), naphtha (N, < 216 °C), and gases (G). Similar to the reaction scheme based on SARA fractions, in this reaction network the cracking of heavier components into lower-molecular-weight fractions is contemplated.

$$\text{Residue} \rightarrow \text{VGO (Reaction 1)} \tag{56}$$

$$\text{Residue} \rightarrow \text{Distillates (Reaction 2)} \tag{57}$$

$$\text{Residue} \rightarrow \text{Naphtha (Reaction 3)} \tag{58}$$

$$\text{Residue} \rightarrow \text{Gases (Reaction 4)} \tag{59}$$

$$\text{VGO} \rightarrow \text{Distillates (Reaction 5)} \tag{60}$$

$$\text{VGO} \rightarrow \text{Naphtha (Reaction 6)} \tag{61}$$

$$\text{VGO} \rightarrow \text{Gases (Reaction 7)} \tag{62}$$

$$\text{Distillates} \rightarrow \text{Naphtha (Reaction 8)} \tag{63}$$

$$\text{Distillates} \rightarrow \text{Gases (Reaction 9)} \tag{64}$$

$$\text{Naphtha} \rightarrow \text{Gases (Reaction 10)} \tag{65}$$

A shallow reservoir with a top depth of 200 m using a grid of 40 × 10 × 30 cells (1, 50, and 1 m in the x, y, and z directions, respectively) was modeled using the STARS of CMG software. Two wells (injection and production) are taken into account at the bottom (producer) with a separation of 5 m (injector). The numerical model is constrained to a minimum pressure of 2164 kPa and a maximum liquid rate of 344 m^3/d for the producer well, as well as a maximum pressure of 2656 kPa and a water rate of 191 m^3/d for the injector well. The quality of steam (at 210 °C) is 95%, which is injected for one year, and then a mixture of steam, hydrogen, catalyst, and vacuum residue is injected for the next 6 years.

To compare injection techniques, such as in situ upgrading technology (ISUT) and steam with a mixture of catalyst, hydrogen, and vacuum residue (ST-ISUT), six cases have been conducted with different injection options. The injectors operate at 210 °C for steam injection and 350 °C for ISUT/ST-ISUT injection during all runs.

Hassanzadeh et al. [38] and Yang et al. [57] conducted a numerical analysis to evaluate the gas production during bitumen recovery using SAGD, solvents, and water-aided electrical heating (SWAEH). A reaction kinetic model was employed (Figure 1i), adapted from Belgrave et al. [75], which consists of eleven components, including coke as the sole solid component. This model integrates thermal cracking and aquathermolysis into three main reactions, enhancing its applicability for reservoir simulation. The reaction network is formulated by combining aquathermolysis and thermal cracking reactions, as follows:

$$\begin{aligned}\text{As} \rightarrow a_{1,1}\text{COKE} + a_{1,2}\text{HO} + a_{1,3}\text{LO} + a_{1,4}\text{H}_2 + a_{1,5}\text{CH}_4 + a_{1,6}\text{CO} + a_{1,7}\text{CO}_2 \\ + a_{1,8}\text{C}_2\text{H}_6 + a_{1,9}\text{C}_3^+ + a_{1,10}\text{H}_\text{S}\text{S}\end{aligned} \tag{66}$$

$$\text{HO} \rightarrow a_{2,1}\text{COKE} + a_{2,2}\text{LO} + a_{2,3}\text{CH}_4 + a_{2,4}\text{C}_2\text{H}_6 + a_{2,5}\text{C}_3^+ \tag{67}$$

$$\text{LO} \rightarrow a_{3,1}\text{COKE} + a_{3,2}\text{CH}_4 + a_{3,3}\text{C}_2\text{H}_6 + a_{3,4}\text{C}_3^+ \tag{68}$$

A robust thermal and reactive multiphase flow simulator (CMG-STARS, 2015 release) was used to model SAGD and solvent and water-assisted electrical heating techniques. The reservoir was represented in a two-dimensional grid (30 m thick, 101 m wide, and 1 km long) with a block size of 1 × 1 m, obtaining 101 and 30 blocks in the x and z directions, respectively. Injection and production wells were centrally positioned, and the reservoir was assumed to have uniform properties: porosity of 0.3, horizontal permeability of 5000 mD, and an anisotropic ratio of 0.45. Initial conditions included a water saturation of 0.15 and an initial temperature of 78 °C. Electrical heaters installed along the wells were designed to effectively heat bitumen, vaporize injected fluids, and mobilize bitumen resources. Each heater had a maximum capacity of 4 kW/m length, contributing to a total energy output of around 346 GJ/day for a 1 km well long. Operational constraints stipulated maximum allowable temperatures of 250 °C for production heaters and 300 °C for injection heaters.

Huang et al. [17] developed a numerical aquathermolysis model that incorporates variations in both gas fractions and heavy oil fractions. The reaction scheme (Figure 1j) depicts the conversion of asphaltene and resin into saturated hydrocarbons, aromatic hydrocarbons, H_2, CO, CO_2, H_2S, CH_4, and HMWG. A numerical reservoir model was developed considering this kinetic model to accurately simulate the heavy oil reservoir. The model comprises 17,280 grids, with 27 grids in the x-direction, 32 grids in the y-direction, and 30 grids in the z-direction. The reservoir properties are characterized by an average effective oil thickness of 124 m, a porosity of 0.281, an oil saturation of 0.7, and an average permeability of 2656 mD. The initial formation pressure was 2550 kPa, and the initial formation temperature was 13 °C.

A numerical reservoir simulation model was developed by Bueno et al. [37] for the in situ aquathermolysis of heavy crude oil with nanocatalysts. The mathematical formulation combines a three-phase equilibrium equation of state, including the mass and energy transport. One important characteristic of this model is that it considers an equation for nanoparticle mass transfer between oil and water, accounting for irreversible and reversible non-equilibrium retention.

$$\tilde{r}_{nano,p\rightarrow rock,ir} = k_{ir,p}\left(1 - \frac{x_{nano,rock,ir}}{x_{nano,rock,ir,eq}}\right)N_{nano,p} \tag{69}$$

$$\tilde{r}_{nano,p\rightarrow rock,rev} = k_{ra,p}\left(1 - \frac{x_{nano,rock,rev}}{x_{nano,rock,rev,eq}}\right)N_{nano,p} - k_{rd,p}N_{nano,rock}\left(\frac{N_p}{N_{oil} + N_{wat}}\right) \tag{70}$$

A five-lump kinetic model (Figure 1k) for aquathermolysis reactions is derived from SARA analysis due to the available thermodynamic properties of these compounds. An important consideration in this model is that since nanocatalysts are focused on the selective adsorption (*ad*) of asphaltene molecules, these are the principal reagent at catalytic aquathermolysis conditions, being the only precursors of gases and maltenes fractions (resins, aromatics, and saturates).

$$As, ad \rightarrow a_1 Re \tag{71}$$

$$As, ad \rightarrow a_2 Ar \tag{72}$$

$$As, ad \rightarrow a_3 Sa \tag{73}$$

$$As, ad \rightarrow a_4 Gas \tag{74}$$

Batch-reactor experiments were performed to optimize kinetic parameters and single-phase core-flooding tests were used to verify nanoparticle retention. The phase transport

parameters were calibrated by reproducing various core-flooding experiments from the literature, and then the results were further up-scaled to laboratory core-scale conditions. For this, a gravel-packed core was simulated with 0.015484 m^2 of length, an effective exposed area of 0.001123 m^2, a porosity of 26.2%, and an initial oil saturation of 78.4%. An injection temperature of 210 °C and a water rate of 0.432 m^3/day were settled. Finally, a field-scale numerical simulation was modeled by scaling up the laboratory parameters. The size of the field in the x, y, and z directions was 91.44, 5.12, and 778.76 m, respectively, with a water injection rate of 10.0321 m^3/d. The rock properties are the same at laboratory- and field-scale: porosity of 26.2%, permeability of 1000 mD, and initial oil saturation of 0.784.

To mitigate the economic drawbacks of SAGD (escalating thermal losses and CO_2 emissions from larger steam chambers), Yang et al. [57] developed a numerical reservoir model. Their work involved a general reaction kinetic model (Figure 1l) for Athabasca bitumen aquathermolysis and thermal cracking, as well as solvent-phase behavior. The findings reveal that their proposed in situ solvent generation enhanced SAGD (ISSG-SAGD) technique offers significant advantages over SAGD, including a 13.77% reduction in steam consumption, an 18.12% decrease in carbon intensity, and a 5.48% increase in oil production. These benefits are driven by two primary factors: the accumulation of non-condensable gases, which diminishes heat loss and maintains reservoir pressure, and the concentration of light hydrocarbons at the drainage interface, which reduces residual oil saturation and enhances drainage rates.

A 2D homogeneous reservoir model for the SAGD approach was developed using the CMG-STARS simulator (2020 release). The model uses a 100 × 1 × 80 grid system representing a reservoir that is 50 m wide and 20 m high. The production and injection wells are positioned 2 m and 7 m, respectively, above the reservoir base. The simulation employs a temperature-independent relative permeability model. The operational parameters include steam at 240 °C and 90% quality. The maximum bottom-hole pressure for the injector is 2730 kPa, and the minimum for the producer is 1500 kPa. A preliminary 4-month steam circulation period is conducted to establish a thermal connection between the injector and producer before the main SAGD operation initiates.

2.4. Main Results of Reservoir Simulations

Numerical reservoir simulation models are vital for evaluating different production strategies and operational scenarios. These tools enable the optimization of oil recovery under aquathermolysis conditions and provide insights into the behavior of steam injection processes. By visualizing simulation data through charts, graphs, and 3D reservoir models, areas for potential improvement can be identified, thus facilitating decision-making in the development and production of heavy oil reservoirs. However, an optimal methodology is crucial to ensure that the predictions match closely with experimental data. Different parameters (oil field properties, operating conditions and modes, and kinetic models) have been studied during the numerical simulation of steam injection technologies, all these factors impact the prediction of oil recovery and production.

Ito and Suzuki [47] conducted an in-depth analysis of the SAGD method, discovering that condensed water primarily displaces oil and transfers energy mainly via thermal convection, which is more efficient than thermal conduction. This process also involves energy loss and steam condensation through both convection and conduction. The natural convection at the upper interface of the steam chamber leads to lower thermal conductivity, prolonging the cooling time of the condensate. Conversely, higher thermal conductivity in the lower reservoir results in increased condensation and shorter cooling time. The oil production rate is influenced by the temperature of the produced fluid, with an optimal subcooling temperature of 36 °C ensuring proper flow between the steam chamber and

the producer. The steam chamber grows predominantly upward and outward due to convective heat transfer and water flow, resembling the expansion of dough in an oven. Based on these outcomes, geomechanical changes within the reservoir are critical using the SAGD method, as they can lead to significant oil loss if the reservoir undergoes a shift, as seen in Figure 2.

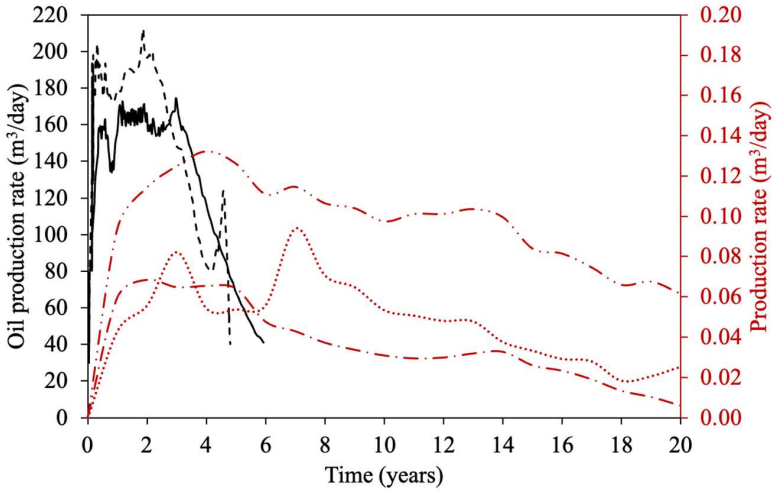

Figure 2. Calculated oil and gas production rate using numerical simulation models without contemplating aquathermolysis reactions. Ito and Suzuki [47], without (solid line) and with (dashed line) considering geomechanical phenomena. Gillis et al. [48] for gas (dotted line), oil (dash-dotted line), and water (dash-double-dotted line) production.

Other parameters, such as relative permeability function and endpoint saturations, significantly influence the shape of the rising steam chamber and cumulative oil recovery, as Sasaki et al. [49] demonstrated (Figure 3). Different permeability (linear and non-linear) functions were employed in this study; however, using linear relative permeability functions with an endpoint saturation different from zero resulted in the shape of a steam chamber like that obtained experimentally. Additionally, heat loss directly affects the prediction of oil production since lower values of this parameter led to earlier well communication, which decreased steam injection requirements and increased oil production.

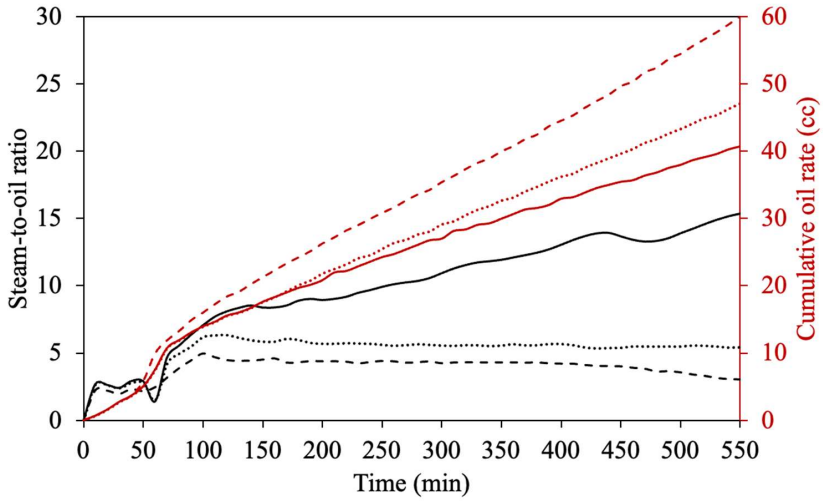

Figure 3. Steam-to-oil ratio and cumulative oil rate obtained for different convective heat transfer coefficients (α) and heat conductivities (λ) values with time, reported by Sasaki et al. [49]. (1) α = 0.041 J/cm^2·min·°C and λ = 0.13 J/cm·min·°C (solid line), (2) α = 0.041 J/cm^2·min·°C and λ = 0 (dotted line), and 3) α = 0 and λ = 0 (dashed line).

The addition of evolved gas composition (using simple kinetic models) has proved to be an important parameter to enhance numerical simulation results. Gillis et al. [48] found that at reservoir conditions, the production rates of CO_2 and H_2S mirrored those of water, consistent with field data showing the presence of H_2S in produced water. Similarly, methane production was correlated with water production, suggesting co-production. The inclusion of gas generation (Figure 2) in numerical simulations significantly reduced bitumen production rates. Simulations with live bitumen (containing gases) showed a larger transition zone, decreasing the efficiency of steam in heating the bitumen and leading to lower oil production rates compared to simulations with dead bitumen (without gases). Despite variations in production rates, the computational effort required for live versus dead bitumen simulations was comparable, indicating the feasibility of incorporating solution gas in SAGD simulations. Similar results were found by Kapadia et al. [52], where the H_2S production increased with steam injection temperature (particularly above 235 °C), affecting the oil production. This is because gases from aquathermolysis reactions impede efficient heat delivery by steam, indicating lower partial steam pressures and large evolved gas pressure within the steam chamber. Therefore, these outcomes indicate that lowering steam injection pressures could improve energy utilization and reduce H_2S emissions. Likewise, Wang et al. [55] noted that including a kinetic model for H_2S production in CSS process simulations improved prediction accuracy. Extended soaking times increased H_2S production, but the rate of increase slowed after the third cycle due to declining oil saturation near the wellbore. Higher steam injection volumes resulted in greater H_2S production due to more intense aquathermolysis reactions.

According to Ibatullin et al. [36], the oil rate peaks when the steam chamber reaches the formation top, with continuous steam injection promoting steam chamber growth and heating larger reservoir sections. When the steam chamber contacts the top of the formation, an increased heat loss to the overburden causes a decline in the oil production rate and a rise in the cumulative steam-to-oil ratio (cSOR). Incorporating gas–water solubilities into the model prevents overestimating gas accumulation and accurately represents H_2S and CO_2 production (Figure 4), avoiding the formation of a large gas cap that impedes heat transfer.

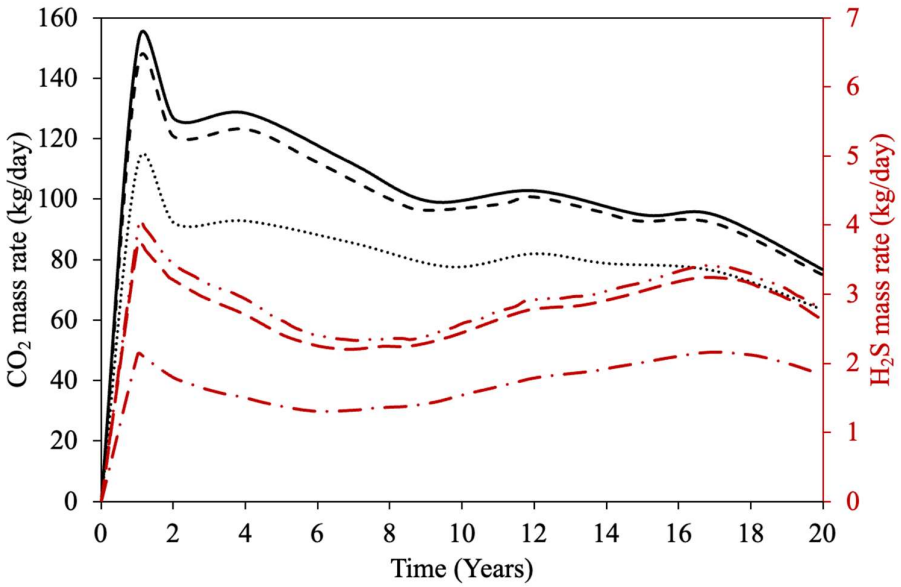

Figure 4. Estimated H_2S (red lines) and CO_2 (black lines) mass rate by Ibatullin et al. [36] for different phases, CO_2 mass rate in oil (solid), CO_2 mass rate in water (dashed), CO_2 mass rate in gas (dotted), H_2S mass rate in oil (dash-dotted), H_2S mass rate in water (long dashed), and H_2S mass rate in gas (dash-double dotted).

Perez-Perez et al. [51] developed a kinetic model that accurately replicated gas plateaus at various temperatures, with an error margin of less than 5% for equilibrium gas emissions. The model showed that gas generation and oil production increase with steam injection pressure (Figure 5), but the steam-to-oil ratio also increases. It was confirmed that the increase in gas production in the reservoir diminishes the oil production rate (above 7 years and 3500 kPa) due to the lower heat transfer from steam to oil provoked by evolved gases. CO_2 production was more temperature-sensitive than H_2S, with higher levels observed at increased temperatures. The model suggests that aquathermolysis reactions primarily occur at the boundaries of the steam chamber, where high temperatures are present. However, the model does not account for interactions between condensate water and acid gases or the dissolution of CO_2 in condensate water, limiting its applicability to different types of heavy crude oils or bitumen.

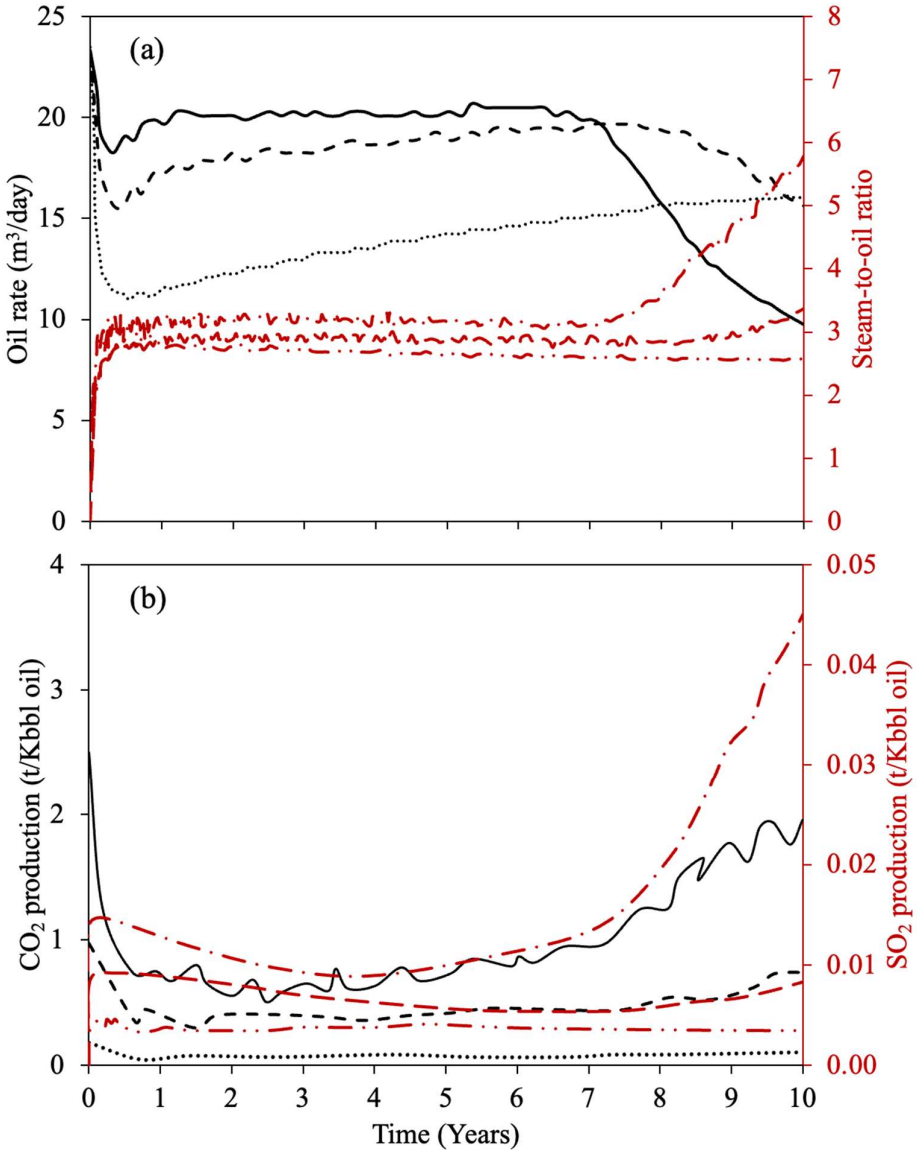

Figure 5. Calculated oil production rate (**a**), steam-to-oil ratio (**a**), and gas production rate (**b**) by Perez-Perez et al. [51] at different pressures. Oil production (black lines) at 3500 kPa (solid), 2500 kPa (dashed), and 1500 kPa (dotted). Steam-to-oil ratio (red lines) at 3500 kPa (dash-dotted), 2500 kPa (long dashed), and 1500 kPa (dash-double dotted). CO_2 production (black lines) at 3500 kPa (solid), 2500 kPa (dashed), and 1500 kPa (dotted). H_2S production (red lines) at 3500 kPa (dash-dotted), 2500 kPa (long dashed), and 1500 kPa (dash-double dotted).

However, these models did not account for changes in components within heavy oil over time. A novel compositional kinetic model was incorporated by Ayache et al. [53] into a reservoir simulation model that accurately replicated changes in H_2S emissions and SARA composition. In this work, different parameters were examined, including the number of cells, the equilibrium constant, and dissolution of H_2S in water/oil. The results showed that a higher number of cells allows higher levels of convergence, especially for short periods. The equilibrium constants (K) remarkably affect the prediction of H_2S production, and thus the dissolution of H_2S because most of the gas produced to the surface is dissolved within water or oil. Another detailed kinetic model was employed by Zhang et al. [16], which evaluates the impact of aquathermolysis reactions in numerical simulations. The findings showed that extended reaction periods aid in converting long-chain compounds into shorter-chain molecules, with gas generation peaking around five days. H_2S concentrations were highest at the top of the reservoir, as well as near the production well for long production periods. A uniform distribution of CO_2 was found for all the reservoirs, heating partially the heavy oil outside the steam chamber, facilitating its extraction. The consideration of aquathermolysis reactions reduced steam partial pressure and increased gas concentrations near the chamber edge, which slowed steam chamber expansion and reduced oil recovery over time, displaying similar to experimental data (Figure 6). Analogous outcomes were obtained by Yuan et al. [54], who demonstrated that numerical models without aquathermolysis reactions initially showed rapid vertical expansion of the steam chamber, followed by predominant lateral growth. In contrast, models with aquathermolysis reactions closely matched experimental temperature distributions, showing restrained vertical expansion and significant lateral growth. The presence of these reactions reduced oil production efficiency over an extended period, attributed to a smaller steam chamber volume and reduced heating due to gas accumulation, which impeded optimal oil recovery (Figure 6).

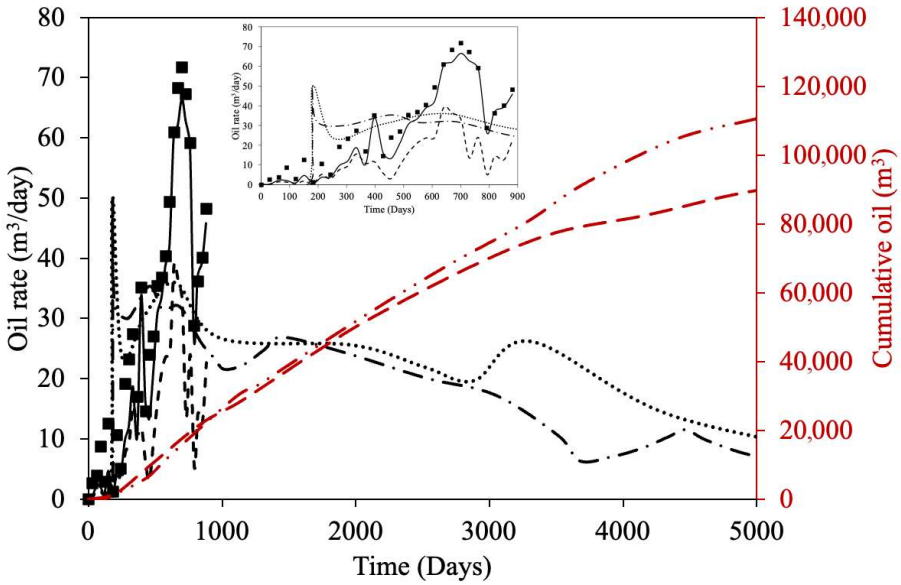

Figure 6. Estimated oil rate and cumulative oil by Yuan et al. [54] and Zhang et al. [16] using numerical simulation models. Oil rate (black lines), historical data (symbols), and calculated by Zhang et al. [16] with (solid) and without (dashed) reactions. Oil rate (black lines) and cumulative oil (red lines) calculated by Yuan et al. [54] with (dash-dotted, long dotted) and without (dotted, dash-double dotted) reactions.

Likewise, Huang et al. [17] reported that incorporating a complex reaction scheme for aquathermolysis further enhances heavy oil mobility by reducing viscosity through com-

positional changes, leading to reduced water production (Figure 7). The steam saturation profiles indicated that higher oil relative permeability and lower water cuts are found close to the wellbore area due to aquathermolysis reactions. In agreement with the previous works that added a kinetic model to the numerical reservoir simulations, the experimental data in this work were more accurately predicted by contemplating a reaction scheme.

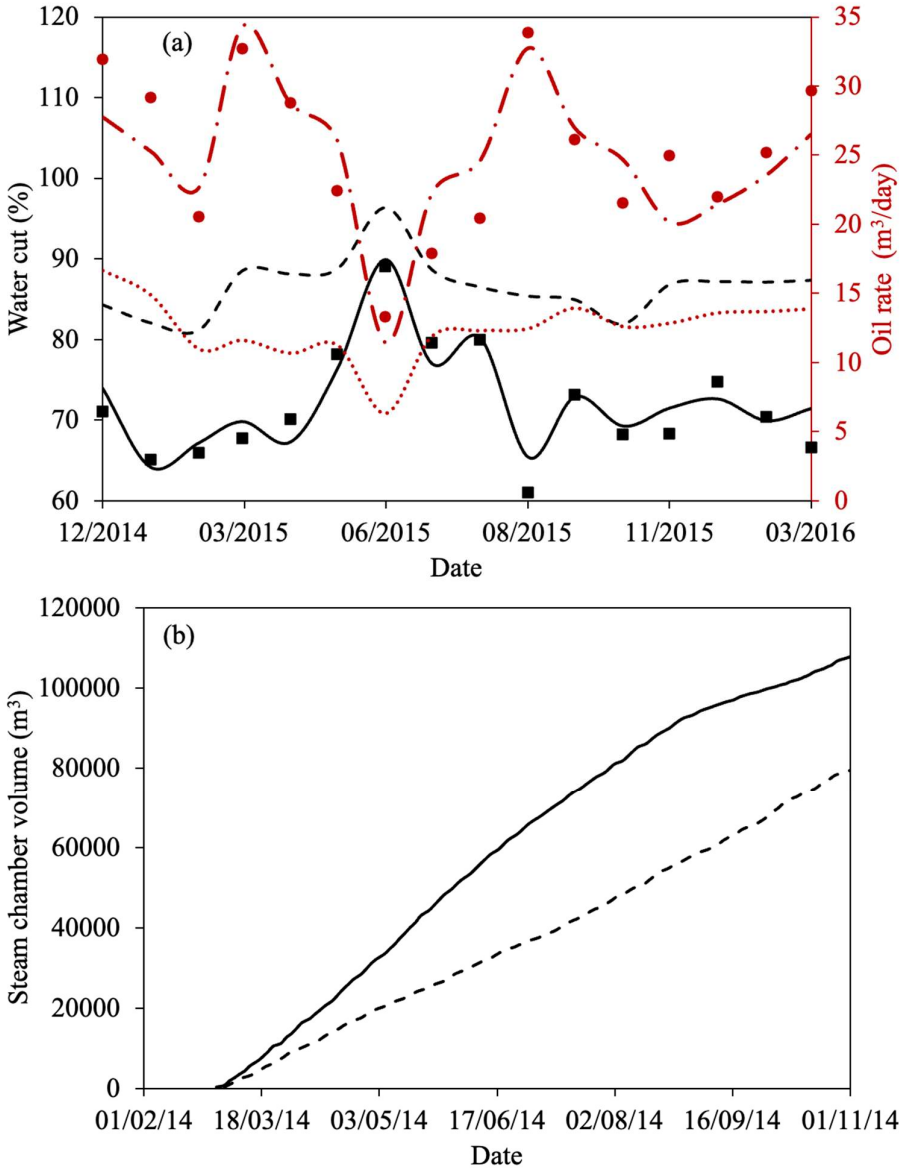

Figure 7. Calculated water cut (**a**), oil rate (**a**), and steam chamber volume (**b**) by Huang et al. [17]. Water cut (black) field data (■) and estimated with (solid line) and without (dashed line) reactions. Oil rate (red) field data (•), and estimated with (dash-dotted line) and without (dotted) reactions. Steam chamber volume with (solid line) and without (dashed line) reactions.

A general kinetic model including the conversion of a hydrogen donor was integrated by Ovalles and Rodriguez [50] in the numerical simulations. A reduction in tetralin conversion from bench- to field-scale was observed during the upgrading process, attributed to poor mixing capabilities of heavy oil and tetralin under reservoir conditions, and the separation of steam by gravity. These interactions, which are difficult to predict at the field scale, diminish the effectiveness of heavy crude oil upgrading and the conversion of tetralin and asphaltenes compared with laboratory-scale results.

An eleven-lump kinetic model was used in a numerical simulation study carried out by Hassanzadeh et al. [38], comparing two injection methods: SAGD and SWAEH. The latter injection approach showed a higher efficiency of water and energy usage, as well as lower coke and gas formation than the former. Additionally, the gas formation does not noticeably affect the oil production during the SWAEH, as it does for SAGD, due to the higher capability of the solvent to dissolve gases and the lower reservoir temperatures. The SWAEH technology is a promising option to eliminate steam plants and reduce water treatment needs, but it needs further studies on geological uncertainties and economic viability.

Another promising option is the use of catalysts to enhance oil recovery. Nguyen et al. [56] found that injecting hydrogen and catalysts with steam significantly reduced oil viscosity, mass density, and residual oil, increasing the VGO, N, and G fractions. The numerical model studied diverse scenarios, varying different parameters and looking for an optimal injection methodology between SAGD and ST-ISUT. It was found for SAGD that the amount of steam remarkably affects the recovery factor, while the ST-ISUT injection method produces more oil with half of the steam-to-oil ratio. Therefore, the ST-ISUT technology diminishes the amount of steam and solvents needed for transportation and upgrading of heavy oil. The addition of catalyst injection to a numerical simulation is not an easy task since it is necessary to account for the dynamic models (transport and retention) due to the complex interactions of water, oil, rocks, and catalyst. Building on experimental studies, the use of nano-sized catalysts for in situ upgrading has shown significant promise. For instance, laboratory work by Bueno et al. [37] demonstrated that injecting nickel-based nanocatalysts during steam injection effectively cracked heavy oil fractions, reducing viscosity by over 80% under controlled conditions. This process relies on the adsorption of heavy components such as asphaltenes onto the catalyst surface, a phenomenon that Bueno et al. [37] showed could be accurately modeled. However, while these laboratory results are compelling, field-scale applications often indicate a lower recovery factor. This performance gap is attributed to upscaling challenges, e.g., steam gravitational segregation, heat loss, and reduced volumetric sweep efficiency, which hinder uniform catalyst-oil contact [76–80]. Consequently, the technology's effectiveness is limited by the predominant interaction of the nano-catalyst with residual oil near the wellbore, leading to a localized piston-like displacement effect rather than widespread reservoir upgrading [81–83].

3. Final Remarks

Significant insights into the optimization of heavy oil recovery are offered by the synthesis of evaluated studies, which analyze the effect of steam injection and aquathermolysis reactions on reservoir performance (Table 1). Initial reservoir simulation models, which omit aquathermolysis reactions, provide a foundational understanding of thermal recovery mechanisms and production optimization strategies. However, the integration of kinetic models significantly enhances predictive capability by accounting for compositional changes in the oil and the influence of in situ generated gases on steam chamber dynamics.

A key advancement is the development of models that combine aquathermolysis with catalytic enhancement strategies, such as catalyst injection or the use of hydrogen-donor solvents, to further increase oil recovery (Figure 8). While these innovative approaches show promise, they also introduce significant scale-up challenges and un-certainties. The dynamic behavior of catalysts and solvents within the heterogeneous reservoir environment is challenging to model accurately and presents a considerable hurdle for field-scale implementation.

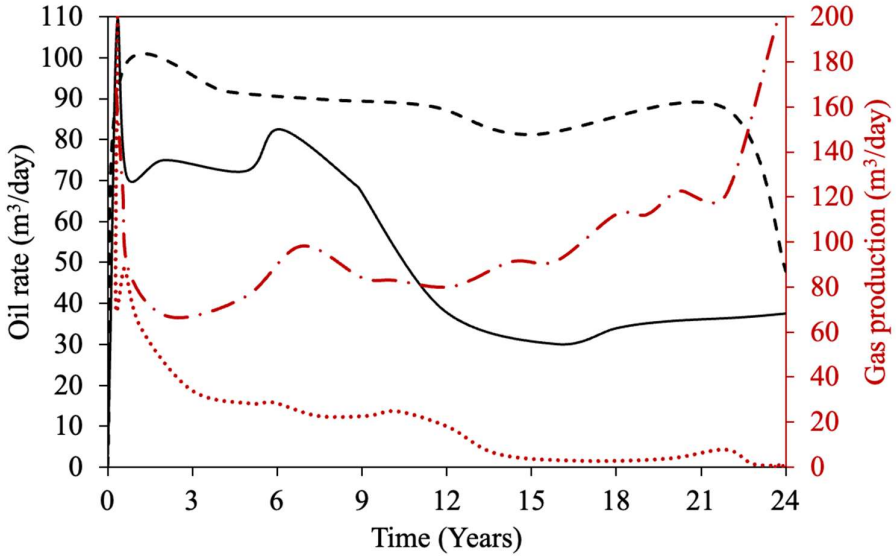

Figure 8. Estimated gas and oil production rate by Hassanzadeh et al. [38] Oil rate with (dashed line) and without (solid line) solvent and water-assisted electrical heating. Gas production with (dotted line) and without (dash-dotted line) solvent and water-assisted electrical heating.

Furthermore, a critical gap in many current models is the omission of long-term catalyst deactivation mechanisms, such as coke deposition, metal sintering, or pore plugging. Failure to account for this deactivation leads to over-optimistic production forecasts and undermines the economic viability of these enhanced recovery methods. Therefore, to improve the accuracy and applicability of reservoir simulations, future work must focus on integrating comprehensive experimental data on catalyst longevity and deactivation, rigorously calibrating models against field-scale pilot data, and validating predictions through scaled physical experiments. Addressing these challenges of scale-up, uncertainty, and catalyst deactivation is crucial for transitioning these promising laboratory-scale insights into reliable and economically feasible recovery strategies.

4. Conclusions

A thorough examination of numerical reservoir simulation studies, including recent advancements, underscored their indispensable role in advancing heavy oil recovery, particularly for aquathermolysis and steam-based techniques. While foundational work established core principles, current research has significantly refined our understanding of in situ upgrading, geomechanics, and the integration of machine learning. These models are crucial for evaluating next-generation production strategies, providing critical insights into complex subsurface dynamics to guide strategic decisions. The key findings of this analysis, updated with the recent literature, are as follows:

- SAGD dynamics and geomechanics: The critical impact of thermal convection on energy transfer remains a cornerstone of SAGD modeling. Recent studies have quantitatively linked geomechanical changes to steam chamber conformance, showing that caprock integrity can be a limiting factor. Furthermore, incorporating non-condensable gas generation from aquathermolysis is now considered essential for accurate production forecasting, as it directly impacts chamber growth and energy efficiency.
- Advanced reaction kinetics and solvent integration: The transition from basic kinetic models to more sophisticated pathways, including coke formation and different gas generation during catalytic aquathermolysis, has highlighted the need for these latter. The synergy between solvents and aquathermolysis has been a major recent focus, with simulations demonstrating that co-injecting light solvents with catalysts can

significantly enhance hydrogen donation and reduce the steam-to-oil ratio (SOR), improving project economics.

- Fluid properties and AI-assisted modeling: The sensitivity of models to relative permeability remains high, increasing the uncertainties of these approaches. A prominent trend since is the application of AI and Machine Learning (ML) to accelerate simulation workflows. These latter are used to optimize well placement and operating parameters in complex, coupled geochemical–geomechanical models, making probabilistic analysis more feasible.
- Emerging hybrid recovery techniques: Hydrogen injection has gained attraction as a method for in situ upgrading with a lower carbon footprint. These simulations consistently show that incorporating the physics of asphaltene adsorption and subsequent permeability alteration is crucial for predicting long-term performance.

Overall, this analysis confirms that the field of numerical reservoir simulation for heavy oil is rapidly advancing. The integration of more sophisticated physics—geochemistry, geomechanics, and advanced fluid behavior—is paramount for enhancing accuracy.

5. Future Research Directions

Building on recent progress, the following avenues are critical for future research:

- Full-physics coupling with AI acceleration: While recent studies have begun coupling processes, future work must achieve full integration of geomechanics, thermal, flow, and complex aquathermolysis kinetics. AI/ML should be leveraged not just as a proxy, but to discover new patterns within simulation and field data that can lead to improved physical models and real-time autonomous optimization.
- High-resolution uncertainty quantification: As models become more complex, the number of uncertain parameters grows. A systematic framework for uncertainties combining high-performance computing with advanced sampling techniques is needed to quantify the reliability of forecasts for these capital-intensive projects, moving from deterministic to probabilistic forecasting.
- Modeling for emissions reduction and sustainability: Future simulations must explicitly track carbon generation and account for the fate of injected gases like hydrogen or CO_2. This will be essential for evaluating the environmental and economic benefits of novel processes, such as catalytic aquathermolysis with carbon capture, utilization, and storage.

By pursuing these directions, the next generation of reservoir simulations will become more predictive, robust, and central to developing the efficient and sustainable heavy oil production strategies demanded by the future energy landscape.

Author Contributions: Conceptualization, G.F. and M.K.; methodology, A.T. and M.K.; software, A.T. and M.K.; validation, M.A.V. and J.A.; formal analysis, G.F., A.T. and J.A.; investigation, G.F. and M.K.; resources, M.A.V.; data curation, G.F. and A.T.; writing—original draft preparation, G.F., A.T. and M.K.; writing—review and editing, M.A.V. and J.A.; visualization, J.A.; supervision, J.A.; project administration, M.A.V.; funding acquisition, M.A.V. All authors have read and agreed to the published version of the manuscript.

Funding: This work was supported by the Russian Science Foundation No. 21-73-30023 (extension) dated 22 May 2025, https://rscf.ru/project/21-73-30023/.

Data Availability Statement: The original contributions presented in this study are included in the article. Further inquiries can be directed to the corresponding author.

Conflicts of Interest: The authors declare no conflicts of interest.

Abbreviations

The following abbreviations are used in this manuscript:

a	Constant for equilibrium correlation (Equation (1))
a_i	The stoichiometric coefficient for component i
A_j	Collision factor for pathway j
Ar	Aromatics
As	Asphaltenes
AQT	Aquathermolysis
b	Constant for equilibrium correlation (Equation (1))
BHP	Bottom hole pressure
c	Constant for equilibrium correlation (Equation (1))
CMG	Computer Modeling Group
COMP1	Single pseudo-component responsible for H_2S production
COMP2	Single pseudo-component responsible for CO_2 production
cSOR	Cumulative steam-to-oil ratio
CSS	Cyclic steam stimulation
D	Distillates
E_{Aj}	The activation energy for pathway j
G	Gases
HCSr	Reactive sulfur species
HMWG	High-molecular-weight gases
HO	Heavy oil
ISUT	In situ upgrading technology
K	Equilibrium constant
k_H	Henry's constant
k_i	Reaction rate coefficient for pathway j
$k_{ir,p}$	Irreversible retention constant
$k_{ra,p}$	Reversible adsorption retention constant
$k_{rd,p}$	Reversible desorption retention constant
LO	Light oil
N	Naphtha
$N_{nano,p}$	Moles of nanocatalyst in phase p
$N_{nano,rock}$	Moles of nanocatalyst in rock
N_{oil}	Number of moles in oil
N_p	Total number of moles in phase p
N_{wat}	Number of moles in water
P	Total pressure
p*	Saturation pressure, KPa
R	Gas constant = 8.314, J/mol-K (Equations (1) and (2))
Re	Resins
Res	Residue
r_i	Reaction rate of component i
$\tilde{r}_{nano,p\rightarrow rock,ir}$	Irreversible non-equilibrium retention
$\tilde{r}_{nano,p\rightarrow rock,rev}$	Reversible non-equilibrium retention
Ru	Universal gas constant
Sa	Saturates
SAGD	Steam-assisted gravity drainage
SF	Steam flooding
ST − ISUT	Steam with a mixture of catalyst, hydrogen, and vacuum residue
STARS	Steam Thermal Advanced Recovery Simulator
SWAEH	Solvent and water-aided electrical heating
T	Temperature
UTCHEM	University of Texas Chemical Compositional

VGO	Vacuum gas oil
$x_{nano,rock,ir}$	Mole fraction of the nanocatalyst in rock that is irreversible
$x_{nano,rock,ir,eq}$	Mole fraction of the nanocatalyst in rock that is irreversible in equilibrium
$x_{nano,rock,rev}$	Mole fraction of the nanocatalyst in rock that is reversible
$x_{nano,rock,rev,eq}$	Mole fraction of the nanocatalyst in rock that is reversible in equilibrium
α	Convective heat transfer coefficient
λ	Heat conductivity
v	Partial molar volume of aqueous solute
γ_g	Activity coefficient of gas solution
ϕ_g	Fugacity coefficient
x_g	Mole fraction of component in water phase
y_g	Mole fraction of component in gas phase

References

1. Abdelsalam, Y.I.I.; Akhmetzyanova, L.A.; Galiakhmetova, L.K.; Baimukhametov, G.F.; Davletshin, R.R.; Dengaev, A.V.; Aliev, F.A.; Vakhin, A.V. The Catalytic Upgrading Performance of $NiSO_4$ and $FeSO_4$ in the Case of Ashal'cha Heavy Oil Reservoir. *Processes* **2023**, *11*, 2426. [CrossRef]
2. Maity, S.K.; Ancheyta, J.; Marroquín, G. Catalytic Aquathermolysis Used for Viscosity Reduction of Heavy Crude Oils: A Review. *Energy Fuels* **2010**, *24*, 2809–2816. [CrossRef]
3. Kapadia, P.R.; Kallos, M.S.; Gates, I.D. A Review of Pyrolysis, Aquathermolysis, and Oxidation of Athabasca Bitumen. *Fuel Process. Technol.* **2015**, *131*, 270–289. [CrossRef]
4. Muraza, O.; Galadima, A. Aquathermolysis of Heavy Oil: A Review and Perspective on Catalyst Development. *Fuel* **2015**, *157*, 219–231. [CrossRef]
5. Speight, J.G. *Enhanced Recovery Methods for Heavy Oil and Tar Sands*; Elsevier: Amsterdam, The Netherlands, 2013; ISBN 0127999884.
6. Dong, X.; Liu, H.; Chen, Z.; Wu, K.; Lu, N.; Zhang, Q. Enhanced Oil Recovery Techniques for Heavy Oil and Oilsands Reservoirs after Steam Injection. *Appl. Energy* **2019**, *239*, 1190–1211. [CrossRef]
7. Tumanyan, B.P.; Petrukhina, N.N.; Kayukova, G.P.; Nurgaliev, D.K.; Foss, L.E.; Romanov, G.V. Aquathermolysis of Crude Oils and Natural Bitumen: Chemistry, Catalysts and Prospects for Industrial Implementation. *Russ. Chem. Rev.* **2015**, *84*, 1145. [CrossRef]
8. Félix, G.; Tirado, A.; Yuan, C.; Varfolomeev, M.A.; Ancheyta, J. Analysis of Kinetic Models for Hydrocracking of Heavy Oils for In-Situ and Ex-Situ Applications. *Fuel* **2022**, *323*, 124322. [CrossRef]
9. Kwofie, M.; Al-Muntaser, A.A.; Varfolomeev, M.A.; Suwaid, M.A.; Yuan, C.; Djimasbe, R.; Saeed, S.A. The Effect of Reaction Time and Temperature on the Aquathermolysis Process of Heavy Crude Oil. *Pet. Sci. Technol.* **2022**, *42*, 514–528. [CrossRef]
10. Vakhin, A.; Sitnov, S.; Mukhamatdinov, I.; Varfolomeev, M.; Rojas, A.; Sabiryanov, R.; Al-Muntaser, A.; Sudakov, V.; Nurgaliev, D.; Minkhanov, I. Improvement of CSS Method for Extra-Heavy Oil Recovery in Shallow Reservoirs by Simultaneous Injection of in-Situ Upgrading Catalysts and Solvent: Laboratory Study, Simulation and Field Application. In Proceedings of the SPE EOR Conference at Oil and Gas West Asia, Muscat, Oman, 21–23 March 2022; p. D012S034R002.
11. Zhao, F.; Liu, Y.; Lu, N.; Xu, T.; Zhu, G.; Wang, K. A Review on Upgrading and Viscosity Reduction of Heavy Oil and Bitumen by Underground Catalytic Cracking. *Energy Rep.* **2021**, *7*, 4249–4272. [CrossRef]
12. Pang, Z.; Jiang, Y.; Wang, B.; Cheng, G.; Yu, X. Experiments and Analysis on Development Methods for Horizontal Well Cyclic Steam Stimulation in Heavy Oil Reservoir with Edge Water. *J. Pet. Sci. Eng.* **2020**, *188*, 106948. [CrossRef]
13. Askarova, A.; Turakhanov, A.; Markovic, S.; Popov, E.; Maksakov, K.; Usachev, G.; Karpov, V.; Cheremisin, A. Thermal Enhanced Oil Recovery in Deep Heavy Oil Carbonates: Experimental and Numerical Study on a Hot Water Injection Performance. *J. Pet. Sci. Eng.* **2020**, *194*, 107456. [CrossRef]
14. Elahi, S.M.; Khoshooei, M.A.; Ortega, L.C.; Scott, C.E.; Chen, Z.; Pereira-Almao, P. Chemical Insight into Nano-Catalytic in-Situ Upgrading and Recovery of Heavy Oil. *Fuel* **2020**, *278*, 118270. [CrossRef]
15. Bueno, N.; Mejía, J.M. Heavy Oil In-Situ Upgrading Evaluation by a Laboratory-Calibrated EoS-Based Reservoir Simulator. *J. Pet. Sci. Eng.* **2021**, *196*, 107455. [CrossRef]
16. Zhang, J.; Han, F.; Yang, Z.; Zhang, L.; Wang, X.; Zhang, X.; Jiang, Y.; Chen, K.; Pan, H.; Lin, R. Significance of Aquathermolysis Reaction on Heavy Oil Recovery during the Steam-Assisted Gravity Drainage Process. *Energy Fuels* **2020**, *34*, 5426–5435. [CrossRef]
17. Huang, S.; Huang, Q.; Liu, H.; Cheng, L.; Fan, Z.; Zhao, L. A Modified Model for Aquathermolysis and Its Application in Numerical Simulation. *Fuel* **2017**, *207*, 568–578. [CrossRef]
18. Yi, S.; Babadagli, T.; Li, H.A. Catalytic-Effect Comparison Between Nickel and Iron Oxide Nanoparticles During Aquathermolysis-Aided Cyclic Steam Stimulation. *SPE—Reserv. Eval. Eng.* **2020**, *23*, 282–291. [CrossRef]

19. Xu, H.; Pu, C. Mechanism of Underground Heavy Oil Catalytic Aquathermolysis. *Chem. Technol. Fuels Oils* **2018**, *53*, 913–921. [CrossRef]
20. Félix, G.; Tirado, A.; Varfolomeev, M.A.; Al-muntaser, A.; Suwaid, M.; Yuan, C.; Ancheyta, J. Chemical and Structural Changes of Resins during the Catalytic and Non-Catalytic Aquathermolysis of Heavy Crude Oils. *Geoenergy Sci. Eng.* **2023**, *230*, 212242. [CrossRef]
21. Tirado, A.; Félix, G.; Varfolomeev, M.A.; Yuan, C.; Ancheyta, J. Definition of Reaction Pathways for Catalytic Aquathermolysis of Liaohe Heavy Crude Oil. *Fuel* **2023**, *333*, 126345. [CrossRef]
22. Li, J.J.; Wang, S.G.; Deng, G.Z.; Tang, X.D.; Yang, Z.; Yang, F.X. Catalytic Aquathermolysis of Heavy Oil by Nickel Ferrite Nanoparticles Prepared via Solvothermal Method. *J. Anal. Appl. Pyrolysis* **2025**, *186*, 106929. [CrossRef]
23. Temizel, C.; Balaji, K.; Ranjith, R.; Coman, C. Optimization of Steamflooding Heavy Oil Reservoirs Under Uncertainty. In Proceedings of the SPE—Asia Pacific Oil and Gas Conference and Exhibition, Perth, Australia, 25–27 October 2016. [CrossRef]
24. Hashemi-Kiasari, H.; Hemmati-Sarapardeh, A.; Mighani, S.; Mohammadi, A.H.; Sedaee-Sola, B. Effect of Operational Parameters on SAGD Performance in a Dip Heterogeneous Fractured Reservoir. *Fuel* **2014**, *122*, 82–93. [CrossRef]
25. Gates, I.D.; Chakrabarty, N. Optimization of Steam Assisted Gravity Drainage in McMurray Reservoir. *J. Can. Pet. Technol.* **2006**, *45*, 54–62. [CrossRef]
26. Yuan, J.; Jiang, R.; Cui, Y.; Xu, J.; Wang, Q.; Zhang, W. The Numerical Simulation of Thermal Recovery Considering Rock Deformation in Shale Gas Reservoir. *Int. J. Heat. Mass. Transf.* **2019**, *138*, 719–728. [CrossRef]
27. Abdulagatov, I.M.; Abdulagatova, Z.Z.; Grigor'ev, B.A.; Kallaev, S.N.; Omarov, Z.M.; Bakmaev, A.G.; Ramazanova, A.E.; Rabadanov, K.M. Thermal Diffusivity, Heat Capacity, and Thermal Conductivity of Oil Reservoir Rock at High Temperatures. *Int. J. Thermophys.* **2021**, *42*, 135. [CrossRef]
28. Chen, Q.; Gerritsen, M.G.; Kovscek, A.R. Effects of Reservoir Heterogeneities on the Steam-Assisted Gravity-Drainage Process. *SPE Res. Eval. Eng.* **2008**, *11*, 921–932. [CrossRef]
29. Le Ravalec, M.; Morlot, C.; Marmier, R.; Foulon, D. Heterogeneity Impact on SAGD Process Performance in Mobile Heavy Oil Reservoirs. *Oil Gas. Sci. Technol.* **2009**, *64*, 469–476. [CrossRef]
30. Deschamps, R.; Guy, N.; Preux, C.; Lerat, O. Analysis of Heavy Oil Recovery by Thermal EOR in a Meander Belt: From Geological to Reservoir Modeling. *Oil Gas. Sci. Technol.* **2012**, *67*, 999–1018. [CrossRef]
31. Huang, S.; Chen, X.; Liu, H.; Xia, Y.; Jiang, J.; Cao, M.; Li, A.; Yang, M. Experimental and Numerical Study of Steam-Chamber Evolution during Solvent-Enhanced Steam Flooding in Thin Heavy-Oil Reservoirs. *J. Pet. Sci. Eng.* **2019**, *172*, 776–786. [CrossRef]
32. Guo, C.; Qu, F.; Liu, Y.; Nian, X.; Chen, Z.; Zou, Y. Numerical Simulation of Steam Injection for Heavy Oil Thermal Recovery. *Energy Procedia* **2017**, *105*, 3936–3946. [CrossRef]
33. Yang, B.; Xu, B.; Yuan, Y. Impact of Thermal Pore Pressure on the Caprock Integrity during the SAGD Operation. *SPE—Heavy Oil Conf. Can.* **2013**, *1*, 744–757. [CrossRef]
34. Zhang, B.; Chalaturnyk, R.; Boisvert, J. Sequentially Coupled Thermal-Hydraulic-Mechanical Simulation for Geomechanical Assessments of Caprock Integrity in SAGD. *Can. Geotech. J.* **2024**, *61*, 1242–1265. [CrossRef]
35. Ayache, S.V.; Lamoureux-Var, V.; Michel, P.; Preux, C. Reservoir Simulation of H2S Production during a SAGD Process Using a New Sulfur-Based-Compositional Kinetic Model. In Proceedings of the SPE—Canada Heavy Oil Technical Conference, Calgary, AB, Canada, 9 June 2015.
36. Ibatullin, T.R.; Yang, T.; Petersen, E.B.; Chan, M.; Rismyhr, O.; Tollefsen, S. Simulation of Hydrogen Sulfide and Carbon Dioxide Production during Thermal Recovery of Bitumen. In Proceedings of the SPE—Reservoir Characterisation and Simulation Conference and Exhibition, Abu Dhabi, United Arab Emirates, 9 October 2011.
37. Bueno Zapata, N.; Morales Mora, O.A.; Mejía Cárdenas, J.M. Practical Kinetic Coupling to Multi-Component and Multi-Phase Flow Transport during in-Situ Heavy Oil Upgrading Processes Using an Equation of State-Based Numerical Reservoir Simulation. In Proceedings of the SPE—Reservoir Characterisation and Simulation Conference and Exhibition, Abu Dhabi, United Arab Emirates, 17 September 2019.
38. Hassanzadeh, H.; Rabiei Faradonbeh, M.; Harding, T. Numerical Simulation of Solvent and Water Assisted Electrical Heating of Oil Sands Including Aquathermolysis and Thermal Cracking Reactions. *AIChE J.* **2017**, *63*, 4243–4258. [CrossRef]
39. Félix, G.; Tirado, A.; Varfolomeev, M.A.; Al-Muntaser, A.; Suwaid, M.; Ancheyta, J. New Approach to Simulate Long-Term in Situ Aquathermolysis Reaction Combining Noncatalytic and Catalytic Kinetic Models. *Ind. Eng. Chem. Res.* **2024**, *16*, 1349–1358. [CrossRef]
40. Song, J.; Yuan, Y.; Gu, S.; Yang, X.; Yue, Y.; Cai, J.; Jiang, G. 2D Numerical Simulation of Improving Wellbore Stability in Shale Using Nanoparticles Based Drilling Fluid. *Energies* **2017**, *10*, 651. [CrossRef]
41. Chekhonin, E.; Romushkevich, R.; Popov, E.; Popov, Y.; Goncharov, A.; Pchela, K.; Bagryantsev, M.; Terentiev, A.; Kireev, I.; Demin, S. Advanced Methods of Thermal Petrophysics as a Means to Reduce Uncertainties during Thermal EOR Modeling of Unconventional Reservoirs. *Geoscience* **2021**, *11*, 203. [CrossRef]

42. Fatehi, H.; Weng, W.; Li, Z.; Bai, X.S.; Aldén, M. Recent Development in Numerical Simulations and Experimental Studies of Biomass Thermochemical Conversion. *Energy Fuels* **2021**, *35*, 6940–6963. [CrossRef]
43. Huang, Z.; Yang, M.; Yang, B.; Liu, W.; Chen, Z. Data-Driven Model for Predicting Production Periods in the SAGD Process. *Petroleum* **2022**, *8*, 363–374. [CrossRef]
44. Cremon, M.A.; Christie, M.; Gerritsen, M.G. Monte Carlo Simulation for Uncertainty Quantification in Reservoir Simulation: A Convergence Study. In Proceedings of the 16th European Conference on the Mathematics of Oil Recovery, ECMOR 2018, Barcelona, Spain, 3–6 September 2018; European Association of Geoscientists and Engineers: Bunnik, The Netherlands, 2018; pp. 1–18.
45. Jaber, A.K.; Al-Jawad, S.N.; Alhuraishawy, A.K. A Review of Proxy Modeling Applications in Numerical Reservoir Simulation. *Arab. J. Geosci.* **2019**, *12*, 701. [CrossRef]
46. Yang, S.; Nie, Z.; Wu, S.; Li, Z.; Wang, B.; Wu, W.; Chen, Z. A Critical Review of Reservoir Simulation Applications in Key Thermal Recovery Processes: Lessons, Opportunities, and Challenges. *Energy Fuels* **2021**, *35*, 7387–7405. [CrossRef]
47. Ito, Y.; Suzuki, S. Numerical Simulation of the SAGD Process in the Hangingstone Oil Sands Reservoir. *J. Can. Pet. Technol.* **1999**, *38*, 27–35. [CrossRef]
48. Gillis, K.A.; Palmgren, C.; Thimm, H.F. Simulation of Gas Production in SAGD. In Proceedings of the SPE/CIM International Conference on Horizontal Well Technology, OnePetro, Calgary, AB, Canada, 6–8 November 2000.
49. Sasaki, K.; Akibayashi, S.; Yazawa, N.; Doan, Q.; Ali, S.M.F. Numerical and Experimental Modelling of the Steam Assisted Gravity Drainage (SAGD) Process. *J. Can. Pet. Technol.* **2001**, *40*, 44–50. [CrossRef]
50. Ovalles, C.; Rodríguez, H. Extra Heavy Crude Oil Downhole Upgrading Using Hydrogen Donors under Cyclic Steam Injection Conditions: Physical and Numerical Simulation Studies. *J. Can. Pet. Technol.* **2008**, *47*, 43–50. [CrossRef]
51. Perez-Perez, A.; Kamp, A.M.; Soleimani, H.; Darche, G. Numerical Simulation of H_2S and CO_2 Generation during SAGD. In Proceedings of the World Heavy Oil Congress, Calgary, AB, Canada, 14 March 2011.
52. Kapadia, P.R.; Wang, J.; Kallos, M.S.; Gates, I.D. Reactive Thermal Reservoir Simulation: Hydrogen Sulphide Production in SAGD. In Proceedings of the SPE—Canadian Society of Unconventional Gas, Calgary, AB, Canada, 15 November 2011.
53. Ayache, S.V.; Lamoureux-Var, V.; Michel, P.; Preux, C. Reservoir Simulation of Hydrogen Sulfide Production during a Steam-Assisted-Gravity-Drainage Process by Use of a New Sulfur-Based Compositional Kinetic Model. *SPE J.* **2017**, *22*, 080–093. [CrossRef]
54. Yuan, R.; Yang, Z.; Guo, B.; Wang, X.; Zhang, L.; Lin, R. Potential Analysis of Enhanced Oil Recovery by Superheated Steam during Steam-Assisted Gravity Drainage. *Energy Technol.* **2021**, *9*, 2100135. [CrossRef]
55. Wang, T.; Yang, R.; Zhang, L.; Zheng, W.; Sun, Y.; Bai, Y. Experimental Measurements and Numerical Simulation of H2S Generation during Cyclic Steam Stimulation Process of Offshore Heavy Oil from Bohai Bay, China. *Appl. Sci.* **2022**, *12*, 7488. [CrossRef]
56. Nguyen, N.; Chen, Z.; Pereira Almao, P.; Scott, C.E.; Maini, B. Reservoir Simulation and Production Optimization of Bitumen/Heavy Oil via Nanocatalytic in Situ Upgrading. *Ind. Eng. Chem. Res.* **2017**, *56*, 14214–14230. [CrossRef]
57. Yang, S.; Huang, S.; Jiang, Q.; Jiang, G.; Zhou, X.; Yu, C. An Innovative in Situ Solvent Generation Enhanced SAGD Technique: Mechanism Analysis Based on Numerical Simulation. *Fuel* **2024**, *364*, 131020. [CrossRef]
58. Hyne, J.B.; Clark, P.D.; Clarke, R.A.; Koo, J. Aquathermolysis—The Reaction of Organo-Sulphur Compounds during Steaming of Heavy Oil | Repository of the Athabasca River Basin. In Proceedings of the 2nd International Conference on Heavy Crude and Tar Sands, Caracas, Venezuela, 7–17 February 1982; Chapter 9.
59. Nie, R.-S.; Wang, Y.-M.; Kang, Y.-L.; Jia, Y.-L. A Steam Rising Model of Steam-Assisted Gravity Drainage Production for Heavy Oil Reservoirs. *Energy Explor. Exploit.* **2020**, *38*, 801–818. [CrossRef]
60. Ovalles, C.; Vallejos, C.; Vásquez, T.; Martinis, J.; Perez-Perez, A.; Cotte, E.; Castellanos, L.; Rodríguez, H. Extra-Heavy Crude Oil Downhole Upgrading Process Using Hydrogen Donors under Steam Injection Conditions. In Proceedings of the SPE international thermal operations and heavy oil symposium, SPE, Porlamar, Venezuela, 12–14 March 2001; p. SPE-69692.
61. Hyne, J.B. *Aquathermolysis: A Synopsis of Work on the Chemical Reaction Between Water (Steam) and Heavy Oil Sands During Simulated Steam Stimulation*; U.S. Department of Energy Office of Scientific and Technical Information: Oak Ridge, TN, USA, 1986.
62. Hyne, J.B.; Tyrer, J.D. *Use of Hydrogen-Free Carbon Monoxide with Steam in Recovery of Heavy Oil at Low Temperatures*; U.S. Department of Energy Office of Scientific and Technical Information: Oak Ridge, TN, USA, 1984.
63. Hyne, J.B.; Clark, P.D. *Additive for Inclusion in a Heavy Oil Reservoir Undergoing Steam Injection*; U.S. Department of Energy Office of Scientific and Technical Information: Oak Ridge, TN, USA, 1985.
64. Clark, P.D. The Behavior of Various Oil Sands towards High Temperature Steam. In Proceedings of the 4th UNITAR/UNDP International Conference on Heavy Crude and Tar Sands, Edmonton, AB, Canada, 7–12 August 1988; pp. 355–367.
65. Good, W.K.; Rezk, C.; Felty, B.D. *Possible Effects of Gas Caps on SAGD Performance.*; U.S. Department of Energy Office of Scientific and Technical Information: Oak Ridge, TN, USA, 1997.

66. Lamoureux-Var, V.; Lorant, F. Method for Constructing a Kinetic Model Allowing the Mass of Hydrogen Sulfide Produced by Aquathermolysis to Be Estimated. U.S. Patent US20070100594A1, 3 May 2007.
67. Lamoureux-Var, V.; Lorant, F. Experimental Evaluation of H2S Yields in Reservoir Rocks Submitted to Steam Injection. In Proceedings of the IOR 2005—13th European Symposium on Improved Oil Recovery, Budapest, Hungary, 25–27 April 2005; European Association of Geoscientists & Engineers: Bunnik, The Netherlands; p. cp-12.
68. Lamoureux-Var, V.; Barroux, C. Using Geochemistry to Address H2S Production Risk Due to Steam Injection in Oil Sands. In Proceedings of the SPE Canada Heavy Oil Conference, SPE, Calgary, AB, Canada, 11–13 June 2013; p. SPE-165437.
69. Kapadia, P.R.; Wang, J.; Kallos, M.S.; Gates, I.D. New Thermal-Reactive Reservoir Engineering Model Predicts Hydrogen Sulfide Generation in Steam Assisted Gravity Drainage. *J. Pet. Sci. Eng.* **2012**, *94*, 100–111. [CrossRef]
70. Kapadia, P.R.; Kallos, M.S.; Gates, I.D. A New Reaction Model for Aquathermolysis of Athabasca Bitumen. *Can. J. Chem. Eng.* **2013**, *91*, 475–482. [CrossRef]
71. Hyne, J.B.; Clark, P.D.; Clarke, R.A.; Koo, J.; Greidanus, J.W. Aquathermolysis of Heavy Oils. *Rev. Tec. INTEVEP* **1982**, *2*, 2.
72. Aliev, F.A.; Mukhamatdinov, I.I.; Sitnov, S.A.; Ziganshina, M.R.; Onishchenko, Y.V.; Sharifullin, A.V.; Vakhin, A. V In-Situ Heavy Oil Aquathermolysis in the Presence of Nanodispersed Catalysts Based on Transition Metals. *Processes* **2021**, *9*, 127. [CrossRef]
73. Vakhin, A.V.; Aliev, F.A.; Kudryashov, S.I.; Afanasiev, I.S.; Petrashov, O.V.; Sitnov, S.A.; Mukhamatdinov, I.I.; Varfolomeev, M.A.; Nurgaliev, D.K. Aquathermolysis of Heavy Oil in Reservoir Conditions with the Use of Oil-Soluble Catalysts: Part I–Changes in Composition of Saturated Hydrocarbons. *Pet. Sci. Technol.* **2018**, *36*, 1829–1836. [CrossRef]
74. Sánchez, S.; Rodríguez, M.A.; Ancheyta, J. Kinetic Model for Moderate Hydrocracking of Heavy Oils. *Ind. Eng. Chem. Res.* **2005**, *44*, 9409–9413. [CrossRef]
75. Belgrave, J.D.M.; Moore, R.G.; Ursenbach, M.G. Comprehensive Kinetic Models for the Aquathermolysis of Heavy Oils. *J. Can. Pet. Technol.* **1997**, *36*, PETSOC-97-04-03. [CrossRef]
76. Xiong, W.; Bahonar, M.; Chen, Z. Development of a Thermal Wellbore Simulator with Focus on Improving Heat-Loss Calculations for Steam-Assisted-Gravity-Drainage Steam Injection. *SPE—Reserv. Eval. Eng.* **2016**, *19*, 305–315. [CrossRef]
77. Chen, F.; Li, M.; Yang, Y.; Zhang, Q.; Lin, N.; Wu, K. Impact of Gravity Segregation on Gas Injection Development in Condensate Gas Reservoirs: A Numerical Simulation Study. *Processes* **2025**, *13*, 1659. [CrossRef]
78. Zafar, A.; Su, Y.; Li, L.; Mehmood, A.; Wang, H.; Fu, J. The Numerical Simulation and Wellbore Modelling of Steam Injection and Stored Heat Recovery from Light Oil Reservoir. *Energy Sources Part. A Recovery Util. Environ. Eff.* **2021**, *43*, 1–16. [CrossRef]
79. Li, H.; Durlofsky, L.J. Upscaling for Compositional Reservoir Simulation. *SPE J.* **2016**, *21*, 0873–0887. [CrossRef]
80. Khalili, Y.; Ahmadi, M. Reservoir Modeling & Simulation: Advancements, Challenges, and Future Perspectives. *J. Chem. Pet. Eng.* **2023**, *57*, 343–364. [CrossRef]
81. Zamani, A.; Maini, B.; Almao, P.P. Propagation of Nanocatalyst Particles Through Athabasca Sands. *J. Can. Pet. Technol.* **2013**, *52*, 279–288. [CrossRef]
82. Zhou, W.; Xin, C.; Chen, Y.; Mouhouadi, R.D.; Chen, S. Nanoparticles for Enhancing Heavy Oil Recovery: Recent Progress, Challenges, and Future Perspectives. *Energy Fuels* **2023**, *37*, 8057–8078. [CrossRef]
83. Soliman, A.A.; Aboul-Fetouh, M.E.; Gomaa, S.; Aboul-Fotouh, T.M.; Attia, A.M. Optimizing In-Situ Upgrading of Heavy Crude Oil via Catalytic Aquathermolysis Using a Novel Graphene Oxide-Copper Zinc Ferrite Nanocomposite as a Catalyst. *Sci. Rep.* **2024**, *14*, 25845. [CrossRef]

Disclaimer/Publisher's Note: The statements, opinions and data contained in all publications are solely those of the individual author(s) and contributor(s) and not of MDPI and/or the editor(s). MDPI and/or the editor(s) disclaim responsibility for any injury to people or property resulting from any ideas, methods, instructions or products referred to in the content.